SOFTWARE TOOL FOR BIOMECHANICAL ANALYSIS OF ELBOW EXTENSION

A SOFTWARE TOOL FOR INTEGRATED BIOMECHANICAL ANALYSIS OF ELBOW EXTENSION

By

JOHN MARKEZ, B.Sc. B.Eng.

A THESIS

Submitted to the School of Graduate Studies

In Partial Fulfillment of the Requirements

For the Degree

Master of Engineering

McMaster University

MASTER OF ENGINEERING (2004)
(Electrical and Computer Engineering)

McMaster University
Hamilton, Ontario

TITLE: A Software Tool for Integrated Biomechanical Analysis of Elbow Extension

AUTHOR: John Markez, B.Sc., B.Eng. (McMaster University)

SUPERVISOR: Dr. H. deBruin

NUMBER OF PAGES: x, 92

ABSTRACT

This thesis describes a software tool used to study the biomechanics of elbow extension. The tool is an integrated computer program for data processing and graphing, and is used in the development of an EMG driven muscle model for dynamic ballistic muscle movement. The software is designed to manipulate data from a series of isometric and dynamic elbow extension experiments. Inputs include recordings from a torque sensor, load cell, and potentiometer as well as EMG from triceps and biceps muscles. Calculations are made to determine the effect of gravity, the Moment of Inertia, as well as the force-EMG, force-length and force-velocity relationships. Additionally, fatigue tests and postactivation potentials are analyzed. Modeling parameters are derived from isometric controls and verified by applying them to data from dynamic experiments.

The principal design requirements for this software tool were adaptability, user control, and data processing protocol verification. The majority of data processing parameters can be controlled and adjusted by the user. Care was taken during software coding so that it would be easy to modify each step of the protocol and if necessary, add additional processing. Data is displayed on interactive graphs to provide control feedback to the user.

TABLE OF CONTENTS

Page

ABSTRACT iii

TABLE OF CONTENTS iv

LIST OF FIGURES vii

LIST OF EQUATIONS ix

LIST OF ABBREVIATIONS x

CHAPTER

1. INTRODUCTION 1

Outline 1
Historical Perspective 2
The Resting Membrane Potential 3
The Nerve Action Potential 6
Mechanism of Muscle Contraction 8
Skeletal Muscle Structure 10
Motor Unit 11

2. STATIC MUSCLE CONTRACTION 13

EMG and Force 13
Analyzing EMG and Force 13
Linear or Higher Order Relationship between EMG and Force 14
Effect of Muscle Fiber Type 15
Effect of Electrode Placement 16
Lack of Experimental Standardization 17
Effect of EMG Processing 18
Effect of Fatigue 18

EMG Processing 19
Smoothing 19
Frequency Analysis of EMG 20
Conclusions for Isometric Contractions 21

3. DYNAMIC MUSCLE CONTRACTION 22

Factors Affecting Force Production during Contraction 22
Basic Biomechanical Factors 22
Force-Length Relationship 24
Force-Velocity Relationship 25
Angle of Muscle Attachment 26
EMG in Dynamic Contractions 27
Dynamic Muscle Models 28

4. SOFTWARE DEVELOPMENT 30

Proposed Solution 31
Measurement System 32
Data Measurement and Recording 35
Project Objective 36
Program Modules 37
Plot and Process Module 39
Gravity and Moment of Inertia Module 45
Gravity and Passive Moment Module Description 47
Moment of Inertia Module Description 49
Mechanical Analysis Module 50
Predict Force from EMG in Static Contractions Module 54
Hill Model Module 61
Dynamic Muscle Model Module 65
Postactivation Potentiation Module 68
Fatigue Module 72
Program Data Module 75

5. DISCUSSION AND CONCLUSIONS 78

Strengths of the Software 78
Limitations of the Software 80
Future Considerations 81

APPENDIX

LABVIEW CODE EXAMPLES 86

Data Flow 86
Data Structures and Functions 87
LIST OF REFERENCES 88

LIST OF FIGURES

Figure page

1-1 Phospholipid Bilayer 4

1-2 The Motor Unit 6

1-3 Typical Transmembrane Action Potential 7

1-4 Sliding Filament Theory 8

1-5 Muscle Structure 10

1-6 Muscle Twitch 12

3-1 Hill Muscle Model 23

3-2 Force-Length Relationship 24

3-3 Force-Velocity Relationship 25

3-4 The Effect of Muscle Angle Attachment 26

4-1 Elbow Extension Apparatus 33

4-2 Data Acquisition and Storage 35

4-3 Torque Predicting Model and Associated Parameters 36

4-4 Plot and Process User Interface Panel 40

4-5 Plot User Selected Data 41

4-6 Load Cell and Torque Meter Signal Processing 42

4-7 Angle Calibration and Preprocessing 43

4-8 EMG Preprocessing 43

4-9 Process all Data from Selected Subject 44
4-10 Gravity and Moment of Inertia User Interface Panel 46
4-11 Compensating for the Effects of Gravity 48
4-12 Calculating the Moment of Inertia 49
4-13 Mechanical Analysis User Interface Panel 51
4-14 Mechanical Output Module Overview 53
4-15 Predict Force from EMG User Interface Panel 55
4-16 Process Triceps EMG 57
4-17 Process Elbow Torque 58
4-18 Calculating Optimum Cuttoff Frequency for Linear Envelope 59
4-19 Hill Model User Interface Panel 62
4-20 Hill Model Module Overview 64
4-21 Dynamic Muscle Model User Interface Panel 66
4-22 Dynamic Model Module Overview 67
4-23 Postactivation Potentiation User Interface Panel 69
4-24 Post Activation Potentiation Module Overview 70
4-25 Fatigue User Interface Panel 73
4-26 Program Data User Interface Panel 76
5-1 User Interface for Proposed Software 82
5-2 Data Flow Diagram for Proposed Software 84

LIST OF EQUATIONS

Equation page

1-1 Goldman Hodgkin Katz Equation 5

4-1 Muscle Model Equation 37

4- 2 True Muscle Torque Equation 47

LIST OF ABBREVIATIONS

AP	Action Potential
ATP	Adenosine Triphosphate
Ca^{+}	Calcium Ion
Cl^{-}	Chloride Ion
CNS	Central Nervous System
CV	Conduction Velocity
EMG	Electromyogram
FG	Fast Glycolytic Muscle Fiber
FOG	Fast Oxidative Glycolytic Muscle Fiber
K^{+}	Potassium Ion
MU	Motor Unit
MUAP	Motor Unit Action Potential
MVC	Maximum Voluntary Contraction
Na^{+}	Sodium Ion
PAP	Postactivation Potentiation
SO	Slow Oxidative Muscle Fiber

> "And truly one can well compare the nerves of the machine that I am describing to the tubes of the mechanisms of these fountains, its muscles and tendons to [diverse] other engines and springs which serve to move these mechanisms, its animal spirits to the water which drives them, of which the heart is the source and the brain's cavities the water main."
>
> 1664 – Traite de l'Homme – René Descartes

CHAPTER 1
INTRODUCTION

Outline

This thesis describes the development of an integrated data analysis tool used in the creation of an EMG driven muscle model for ballistic elbow extension. The following text not only illustrates the functionality and interactive capabilities of the software, but explains how the program and muscle model co-evolved.

The author wishes to demonstrate that this thesis is greater than its end product. The development of the resulting software required background knowledge of muscle physiology, a practical understanding of experimental limitations with electromyography, as well as the technical expertise to create a functional and dynamic software tool. This document is organized in that spirit. Chapter One gives a historical account of relevant work in conjunction with a brief discussion of background physiology. Chapters Two and Three discuss the practical considerations involved in using electromyography in muscle models for static and dynamic contractions. Chapter Four describes the structure of the program, focusing primarily on data flow and user interactivity. Finally, Chapter

Five discusses the strengths and limitations of the program and makes suggestions for possible future work.

Historical Perspective

Speculation as to the function of the nervous system can be traced as far back as Aristotle (384-322 BC). He and others like Galen (129-210 AD) envisioned a body that worked on hydraulic principles. The brain was considered to be the "seat of the soul" and the brain's ventricles, reservoirs of "animal spirits". Nerves served as conduits of these spirits which were necessary for the functioning of the whole body.

The great French naturalist and philosopher René Descartes (1596-1650) suggested that the nerves conducted stimuli from the brain. Though still accepting the model on its hydraulic principles, he correctly conceived the idea of the 'reflex arc', and the nerves' function to transport stimuli from sense organs to the brain, as well as motor activation stimuli from the brain to the muscles.

It was not long however before the experimental scientists took over from the philosophers. Luigi Galvani (1737-1798), while dissecting a frog, discovered that he could cause the animal's leg to move by touching the muscle's nerve with his knife. He performed a number of experiments in which he elicited contraction from various animal muscles. Galvani believed that muscle tissue was capable of generating a type of "animal electricity". Alessandro Volta (1745-1827) rejected this idea and correctly postulated that the electricity was generated via the contact of two different metals: the scalpel and the dissecting pan. This electricity, he suggested, traveled through the nerves and caused the muscles to contract. The nature of this "current" however was not understood. Was

it the same movement of free electrons as in conducting metal wires? Herman von Helmholtz showed in 1852 that the conduction velocity (CV) along the nerve was far too slow to be explained by a flux of free electrons.

Between 1881 and 1887 Sydney Ringer performed a series of experiments on ions and frog heart function. Ringer discovered that ions of Sodium, Potassium and Calcium were all required to be in solution in specific relative concentrations in order for the frog heart to work.

The term Action Potential (AP) was first used by Julius Bernstein in 1902 to describe the self perpetuating depolarization and subsequent repolarization of excitable cell membranes.

In 1913 Edgar Douglas Adrian discovered that nerve signals were transmitted as pulses as opposed to continuous waveforms. He subsequently received the 1932 Nobel Prize in Physiology and Medicine for his discovery.

The stage was finally set for the birth of neurophysiology

The Resting Membrane Potential

To an electrical engineer, perhaps the most fascinating aspect of physiology is the magnitude of the potential gradient across excitable membranes. The electrochemical voltage across such membranes is approximately 90 mV. When it is considered however, that this difference exists across a distance of only five to ten nanometers, the resultant gradient is on the order of one million volts per meter. It is not surprising to discover that

the resting membrane potential plays a pivotal role in many cellular functions including membrane transport, nerve conduction and specific to this study, muscle contraction.

The membrane of a cell is composed of a bilayer of phospholipid molecules. These molecules are composed of a hydrophilic head and two hydrophobic fatty acid tails. When arranged with their tails facing one another, the molecules form a hydrophobic barrier that is not easily penetrated by either water or solute particles. The configuration of the phosopholipid bilayer is shown in Figure 1-1.

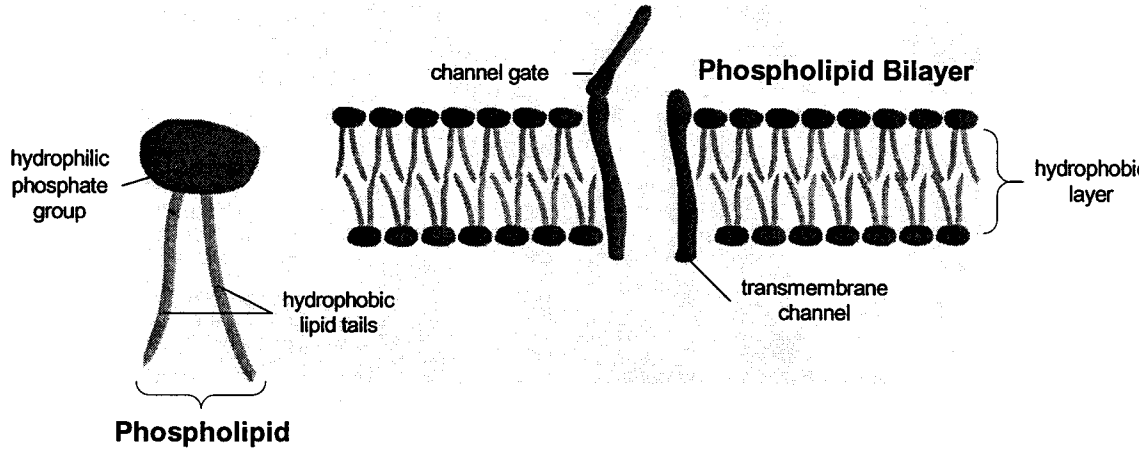

Figure 1-1 Phospholipid Bilayer

This bilipid arrangement is fundamental to all animal cell membranes. Transport into and out of the cell is managed via channels which are for the most part gated and controlled by various means such as the potential across the bilipid layer, or the concentration of "key" ligand particles.

At equilibrium, ions exist on either side of the membrane in unequal concentrations. This results in a concentration gradient across the membrane. The charged nature of ions results also in an electrical or charge gradient. These two

gradients balance one another subject to the membrane's relative permeabilities to constituent ions. Sodium (Na^+), Potassium (K^+) and Chloride (Cl^-) are the principle contributors to these gradients. The 'Goldman-Hodgkin-Katz' equation can be used to predict the potential inside the cell relative to the outside if ion concentrations and their membrane permeabilities are known.

$$E_m = \frac{RT}{F} \cdot \ln \frac{P(K^+) \cdot [K+]_o + P(Na^+) \cdot [Na^+]_o + P(Cl^-) \cdot [Cl^-]_i}{P(K^+) \cdot [K+]_i + P(Na^+) \cdot [Na^+]_i + P(Cl^-) \cdot [Cl^-]_o}$$

R	=	Molar gas constant (8.314 J/mol·K)
T	=	Absolute temperature
F	=	Faraday's constant (96485.3 C/mol)
[ion]	=	Concentration of ion
P(ion)	=	Permeability of membrane to ion
Na^+	=	Sodium ion
K^+	=	Potassium ion
Cl^-	=	Chlorine ion

Equation 1-1 Goldman Hodgkin Katz Equation (Mullins and Noda, 1963)

The Nerve Action Potential

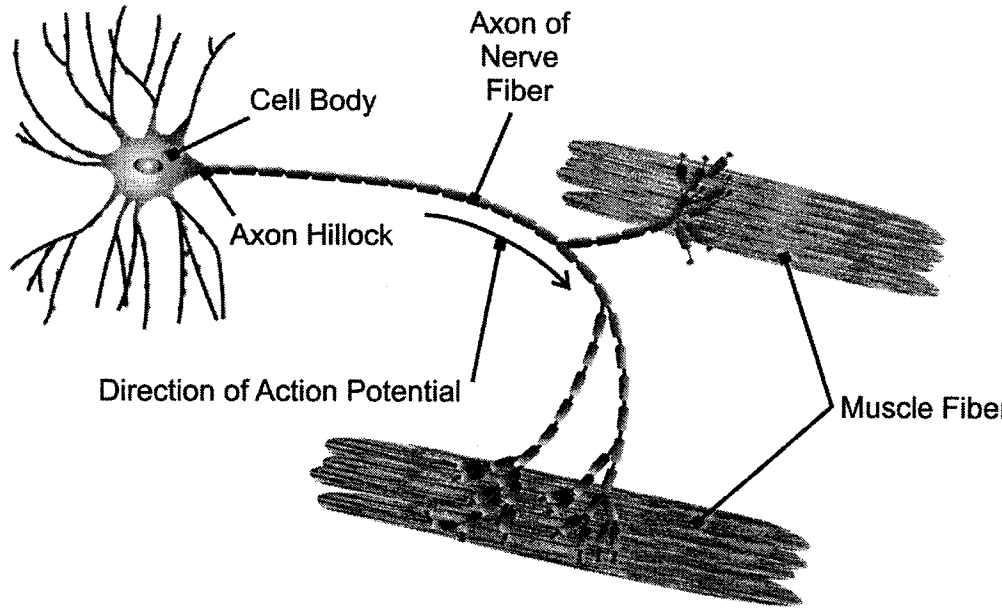

Figure 1-2 The Motor Unit

A signal is transmitted via a nerve cell by an event referred to as the Action Potential. Figure 1-2 depicts a nerve cell and its associated muscle fibers. An Action Potential is generated at the cell body and travels the length of the axon towards the innervated muscle fibers. This event is initiated when a variety of membrane depolarizing events cause the membrane potential at the Axon Hillock to exceed a threshold value of -55 mV. Action Potentials are characterized by a sudden depolarization and subsequent repolarization of the nerve membrane. This localized event occurs in less than one millisecond, yet it is self-propagating because it initiates the depolarization of neighboring membrane. It is an "all or none" binary event.

In terms of nerve fiber "signal", there is no information in the amplitude or the shape of an Action Potential. The depolarization occurs when gated channels suddenly open causing the membrane to become highly permeable to Na^+. These positively charged ions flow into the cell and change the potential from approximately -90 mV to +35 mV as shown in Figure 1-3. Within a fraction of a millisecond, the Na^+ channels close and K^+ channels open. Both these events serve to repolarize the membrane to its original resting potential. It is this depolarization and subsequent repolarization which travels the length of the nerve fiber and is the "signal" which is transmitted by the nerve. Its propagation relies on voltage-gated Na^+ channels which open when the nearby potential rises above the threshold value. Since it is an *all or none* event, the information is not coded in the amplitude but rather by the timing and frequency of successive firings.

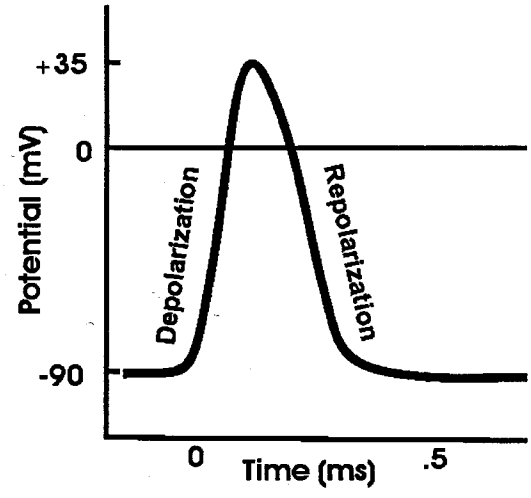

Figure 1-3 Typical Transmembrane Action Potential

Mechanism of Muscle Contraction

The contraction of a muscle fiber begins with the transmission of an Action Potential along an α-motor neuron. The Action Potential, when it reaches the nerve endings causes a release of acetocholine into the synaptic cleft which separates the nerve from the fiber it innervates. Acetocholine-gated Na^+ channels open, causing depolarization and initiation of an Action Potential along the membrane of the muscle fiber. This signal travels along the membrane and deep into the muscle cell via T-tubules to depolarize the Sarcoplasmic Reticulum which subsequently releases its store of Calcium ions (Ca^+) into the myofiber space. Calcium causes conformational changes in troponin-c which exposes the actin filament binding sites and allows the interaction of actin and myosin and the subsequent contraction of the muscle fiber.

Myofibril shortening is generally explained via the Sliding Filament Theory.

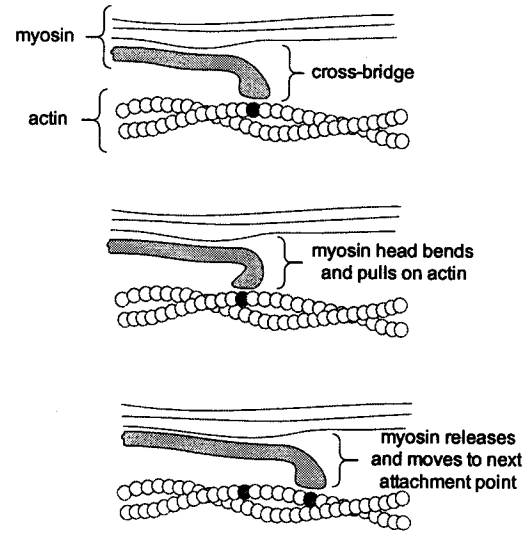

Figure 1-4 Sliding Filament Theory

Contraction occurs when head-like structures on the thicker myosin fibers pull on adjacent actin filaments as shown in Figure 1-4. These head like structures form temporary cross-bridges with activated actin filament sites. They attach, pull, release and then repeat the process further along the filament. This "ratcheting" slides the filaments past one another thereby shortening the myofiber. The collective effect of myofibril shortening is contraction of the entire muscle.

Limb movement, such as forearm flexion, depends not only on the organized contraction or twitch of muscle fibers, but on the interplay of connective tissue, force transfer through skeletal attachments and the coordination of several muscles.

Skeletal Muscle Structure

Skeletal muscle is organized into a hierarchy of fiber groupings as shown in Figure 1-5.

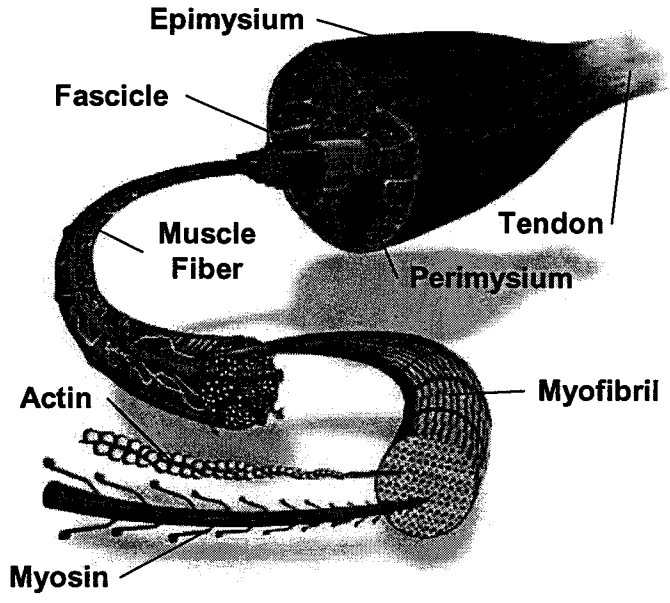

Figure 1-5 Muscle Structure (P. Joachim – www.artwiredmedia.com)

The fundamental structural units are the actin and myosin myofibrils which are arranged longitudinally and shorten or contract the muscle cell to which they belong. Muscle cells are also referred to as fibers as they generally run along the length of the muscle and are attached to tendon at both ends. They each contain an ordered structure of myofibrils as well as other cell organelles common to all somatic cells such as mitochondria, nuclei, and sarcopalsmic reticulum. It is interesting to note that skeletal muscle cells contain many mitochondria as well as multiple nuclei in order to provide sufficient energy and protein production capacity for these active cells. Muscle fibers are arranged in bundles or fascicles separated by sheaths of connective tissue called

perimysium. These fascicles are further grouped and surrounded by epimysium to form the whole muscle structure.

Motor Unit

The fundamental element of muscle control is the Motor Unit (MU). First named by Nobel laurite Charles Scott Sherrington (Sherrington 1925), it is composed of all the muscle cells which are innervated by an α-motor neuron as well as the neuron itself. A diagram can be seen in Figure 1-2. Following the "all or none" principle, the discharge or activation of the α-motor neuron leads to the near simultaneous contraction of its associated muscle cells. Skeletal muscles are composed of a non-contiguous distribution of hundreds of these MUs (Bodine-Fowler et al. 1990). Furthermore, the spatial territories of these distributions differ widely between MUs (Buchtal, Guld and Rosenfalck 1957). An overall smooth muscle contraction results from the asynchronous firing of recruited MUs. A one time activation from a single MU would result in a small muscle twitch as the one shown in Figure 1-6. During normal contraction, MUs fire continuously, at a near constant rate. Other MUs will fire with their own rate and phase. These twitches summate at the tendon, which transmits the force of the attached fibers causing an overall smooth contraction.

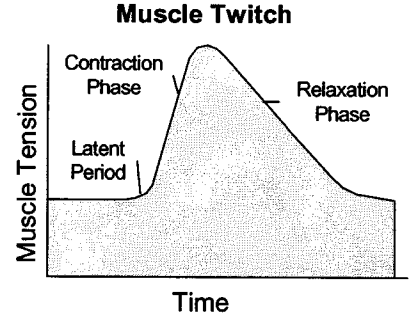

Figure 1-6 Muscle Twitch

The Central Nervous System (CNS) employs two methods to vary the forces generated by a muscle. The first is called "recruitment" and refers to control over the number and order of MUs which are activated (Gilson and Mills 1941). Gilson and Mills explain that during a gradually increasing voluntary effort, MUs are recruited in order of their relative thresholds. The second method, "rate modulation", refers to control over the rate and pattern of MU activations (Adrian and Bronk 1929) (Person and Kudina 1972). The CNS increases generated muscle force via a combination of increased MU recruitment and increased rate modulation. The relative contribution of each method depends on muscle type, degree of force, and type of muscle contraction.

CHAPTER 2
STATIC MUSCLE CONTRACTION

EMG and Force

The electromyogram (EMG) is a complex signal. It is the summation of all Motor Unit Action Potentials (MUAP) that are detected by recording electrodes prior to and during the contraction of a muscle. Muscle fiber tissue depolarization generates an electro-chemical signal that is transmitted to electrodes which in turn generate minute electrical currents that can be amplified and then analyzed. In a similar way that many individual fiber twitches summate at the tendon to yield a whole muscle force, multiple MUAPs summate at the skin electrode to yield an EMG signal. The degree to which each MUAP is distorted or filtered depends not only on its distance and orientation with respect to the electrodes but to the dielectric properties of the muscle and associated tissues within the detection area.

Analyzing EMG and Force

Both force and EMG recordings are measures of muscle activity. We generally consider that the purpose of a muscle is to generate force, thus we evaluate a muscle's performance by the amount of force it can produce as well as the duration, resistance to fatigue and frequency with which it can produce such forces.

In most situations, we are concerned with the torque produced through a joint, such as an arm flexion or a knee extension. These movements depend on the interaction of more than one contracting muscle. In the case of human locomotion, dozens of muscles are involved. It is practically impossible to non-invasively measure the force or performance of an individual muscle using force transducers alone. The situation becomes especially complicated for dynamic contractions.

Since EMG is an indication of muscle activity, it is often used as an indirect predictor of force, and for decades researches have been attempting to characterize the relationship between the two. To be sure, a surface EMG signal when rectified and smoothed is approximately related to the amount of force produced by the muscle. However, there is no convenient mathematical analysis or computational transform that can be universally applied.

Linear or Higher Order Relationship between EMG and Force

Original studies showed no correlation between muscle tension and its recorded twitch potential (Rosenblueth, Wills and Hoagland 1941). Lippold, in 1952, was the first to show a linear relationship between force and integrated EMG for voluntary plantar flexion. He noted that integrated EMG took into account the number of active motor units as well as the frequency of their firing (Lippold 1952). Inman et al. also found such a "parallel" relationship in the biceps muscle (Inman et al. 1952).

At the same time, an increasing number of studies reported more complex, higher order relationships between force and EMG (Zuniga and Simons 1969) (Lindström, Magnusson and Petersén 1974)

There are a wide variety of factors responsible for such conflicting results. Experimental conditions, EMG recording method, post recording signal processing, and even variations in physiology each contribute to obfuscating the true relationship between processed surface EMG and force output.

Effect of Muscle Fiber Type

There exist at least three distinct classes of MUs based on the functional (Burke et al. 1973) and metabolic (Brook and Kaiser 1970) properties of their constituent muscle fibers: slow oxidative (SO), fast oxidative glycolytic (FOG) and fast glycolytic (FG). The SO fibers have long isometric twitch durations and low shortening velocities, yet are highly resistant to fatigue as they have a high mitochondrial content. The fast fibers have short twitch durations and high shortening velocities. The two fast types are distinguished from one another by their metabolic properties. FOGs like SOs, also have many mitochondria and employ oxidative phosplorylation to provide energy for fiber contraction. FGs, on the other hand, are much more subject to fatigue due to their primary reliance on glycolysis.

Effect of Electrode Placement

EMG is collected via bipolar surface electrodes and amplified using a differential amplifier. In order to detect a single event such as an Action Potential traveling the length of a muscle fiber, the signal must reach each electrode pole with a different phase. This occurs when each pole of the electrode is a different distance from the Action Potential. Maximum difference in phase will occur when the poles are arranged in parallel and directly over the muscle fiber. It is easy to see that the signal would be completely rejected if the poles were arranged transversely and bisecting the muscle fiber axis. Thus, any deviation from the parallel position directly over the activated fiber results in a decrease in EMG signal.

It is also important to consider electrode placement with respect to fiber innervation zone (Buchthal, Guld and Rosenfalck 1955). If the poles of the recording electrode are placed in such a way as to straddle the motor endplate, signals with very similar characteristics would reach each pole and thus be rejected by a differential amplifier. Multiple innervation zones may exist, and their locations may vary between individuals for the same muscle (Masuda, Miyano, Sadoyama 1985).

As previously discussed, EMG is not the result of only one Action Potential from a single uniform muscle fiber. It is the result of activation from motor unit pools of different size, orientation and distribution. Furthermore, it must be considered that the signal conduction medium is not uniform, thus affecting the relative dispersions of different MUAPs (Gootzen, Stegeman and Van Oosterom 1991) (Gydikov 1981) (Gydikov et al. 1984) (Broman, Bilotto and De Luca 1985). For example, muscle tissue

is nonhomogeneous and anisotropic with the impedance in the direction of the fiber considerably less than that in the transverse direction. Thus, the conduction medium of the muscle tissue itself distorts signals that travel through it by the degree of its irregularity. As well, blood vessels have low impedance, while subcutaneous fat has high impedance. The resulting signal is distorted from that recorded from an idealized homogeneous isotropic infinite volume conductor (Buchthal, Guld, and Rosenfalck 1954) (Buchthal, Pinelli, and Rosenfalk 1954) (Dumitru and DeLisa, 1991).

Lack of Experimental Standardization

Most early studies held the following factors responsible for conflicting results: variation in electrode type, electrode placement, tissue preparation, selected muscle type, and fatigue. It is quite impossible to control for all these factors. For practical collection of surface EMG, the muscle must be treated as a single unit, and assumptions made about its orientation, and innervation zone with respect to electrodes. As well, uniformity must be assumed in MU distribution and signal volume conduction. Still, it remains very difficult to standardize experiments from one subject to the next, and nearly impossible for experiments in different labs using a variety of measuring equipment. Even when the above factors can be controlled for as in the case of repeated recording from the same subject, variations still occur (Siegler, 1985).

Siegler et al. hypothesized that the localized nature of EMG recordings is primarily responsible for significant intra-subject variability. Small variations in spatial motor unit recruitment patterns, though they may have little or no impact on force production, can

dramatically affect recorded EMGs. There are in fact a number of patterns available to the CNS to activate the motor unit pool (Kernell 1992). Also, motor units may also be rotated from a recruited to a de-recruited state throughout activation (Person 1974) (Enoka, Robinson and Kossev 1989). In addition to variations in spatial activation strategies, variations in rate modulation can also have a significant affect on measured EMG (Kukulka and Claman 1981).

Effect of EMG Processing

To complicate matters further, the chosen method of EMG processing can greatly affect final results. Siegler et al., for example, show that even during identical experimental setups and under carefully controlled contractions, the relationship between torque and EMG can be anything from linear to higher order, depending only on the selected method of EMG processing (Siegler et al. 1985).

Effect of Fatigue

Fatigue is commonly defined as the decrease in capacity to produce a desired force. The onset of fatigue manifests itself in the EMG signal as a change in component frequency spectrum. As the level of fatigue increases, the resulting EMG spectrum compresses and the centroid frequency shifts to a lower value. Firstly, the concentration of lactic acid increases with greater fatigue. This causes a slowing of conduction velocity, resulting in longer signal time constants and a lower frequency spectrum. Furthermore, alteration in CNS recruitment strategy can also contribute to the shift in

spectrum. Additionally, fatigue is dependent on fiber type. Fast Glycolytic muscle fibers for example are more subject to fatigue. (Hamm, Reinking and Stuart 1989). Fatigue can be the manifestation of a decrease in neural output, known as central fatigue or a decrease in output of contractile components known as peripheral fatigue. Finally, the effects of fatigue can be both short and long lasting (Edwards et al. 1977).

EMG Processing

EMG is typically characterized by its amplitude and by its frequency spectrum. Techniques such as peak to peak amplitude measurements or counting the number of peaks exceeding an arbitrary threshold value try to capture both amplitude and frequency information. Today, the most common EMG analysis begins with full wave rectification of the amplified signal followed by integration over a window of time.

Smoothing

Typically, a linear envelope is obtained from the rectified signal by feeding it through a low pass filter with a sufficiently low cutoff. When properly tuned, this envelope encapsulates the original rectified EMG and bears a striking resemblance to force recordings from the same muscle contraction. At the very least, such an envelope provides a visually appealing indication of overall muscle activity.

The amplitude of this envelope is proportional to the number of MUs firing, their amplitude, and rate of firing over a window of time subject to the principle of superposition and attenuation based on the medium through which they travel.

Traditionally, a second order Butterworth filter has been used to accomplish the task of producing such envelopes.

As would be expected, low pass filtering can introduce a phase lag to the envelope with respect to the original waveform. This lag can be minimized by using a critically damped filter tuned to the characteristics of a muscle twitch. Fuglevand et al., for example, modeled MU twitch force as an impulse response of a critically damped second order system (Fuglevand, Winter and Patla 1993).

Often, cutoff frequency is selected based on the rise time of selected muscle twitch (Hof and Berg 1981a). An alternate approach to minimizing the effects of phase lag is to reverse the waveform and pass it through the filter a second time.

Frequency Analysis of EMG

Spectral analysis of EMG can yield more telling information than just the overall muscle activation. It can be used to indicate onset as well as the degree and nature of muscle fatigue. Shifts in the EMG spectrum can be detected even before a muscle loses its ability to maintain a given force.

Each MUAP has unique frequency characteristics. MU size, shape and distance from recording electrodes all contribute to the overall EMG spectrum. Thus, different recruitment strategies will result in different spectra. Additionally, rate modulation of each motor unit will have its own effect. Clearly, a great deal of information is contained within the frequency distribution of EMG. The key to meaningful analysis is extraction of information that is relevant to one's particular objective.

Conclusions for Isometric Contractions

Complications, variations, and a seemingly endless list of mitigating factors can discourage even the most persistent experimental scientist and diminish any hope of finding a meaningful relationship between force and EMG. Still, because EMG is so easy to record, it remains the most ubiquitous diagnostic tool in neuromuscular physiology (De Luca 1997).

Given proper assumptions and strict experimental controls, EMG analysis has yielded generally accepted measures of muscle activation for isometric contractions. Dynamic contractions are an entirely different story however as will be discussed in the next chapter.

CHAPTER 3
DYNAMIC MUSCLE CONTRACTION

The majority of muscle activity in real life is dynamic. A large amount of research is focused on exploring the relationship between dynamic muscle contraction and joint biomechanics. Many problems arise when trying to characterize this relationship. Factors such as joint angle, muscle length, shortening velocity, the three dimensional structure of the muscle, muscle group co-ordination, and the effect of gravity on different limb orientation, bone, ligament and tendon forces all help to cloud the relationship.

Factors Affecting Force Production during Contraction

Basic Biomechanical Factors

To modern biomechanists, A. V. Hill is considered to be the father of muscle modeling. Hill used an improved combination of thermopile and galvanometer to measure the heat produced by muscles as they shorten (Hill 1937). He developed a model based on the energetics of contraction (Hill 1938). Hill conceived three modeling parameters, a contractile component, or undamped element along with two elastic elements: one in *series* and one in *parallel*. The components of his model depend on force-length and force-velocity relationships.

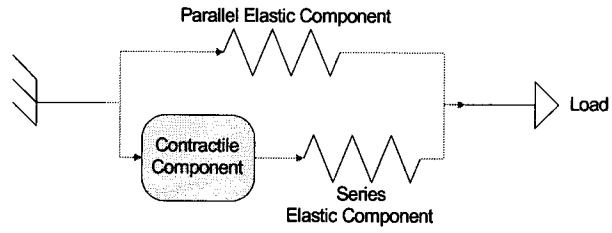

Figure 3-1 Hill Muscle Model

Physical explanations for these relationships however had to wait for the sliding filament theory. A. F. Huxley and Niedergerke as well as H. E. Huxley and Hanson independently discovered that thick myosin and thin actin filaments, which are the constituent components of muscle tissue, slide by one another when the muscle contracts. (Huxley and Niedergerke 1954) (Huxley and Hanson 1954). They used an interference microscope and a phase-contrast microscope respectively to make their discoveries. These ideas were later formulated into a mathematical model (Huxley 1957). Huxley and Simmons developed the actual model for these *sliding* filaments (Huxley and Simons 1971) that is still used today. In it, they explain how the cross-bridges actually produce force between actin and myosin. This model, as well as the associated hydrolysis of ATP, is one of the most exhaustively studied subjects in muscle biochemistry.

Force-Length Relationship

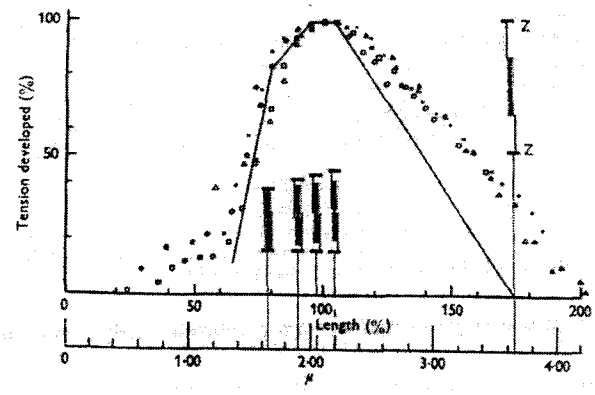

Figure 3-2 Force-Length Relationship (Gordon 1964)

The magnitude of force that a muscle can produce depends on its length. Maximum tension can be developed when a muscle is at optimal conditions for actin and myosin interaction. At this muscle length, filaments are aligned so that the most number of cross-bridges can form. At shorter muscle lengths, the filaments exceed their ability to overlap resulting in a decreased capacity to generate tension. At longer lengths, fewer cross-bridges can form due to less filament overlap.

Force-Velocity Relationship

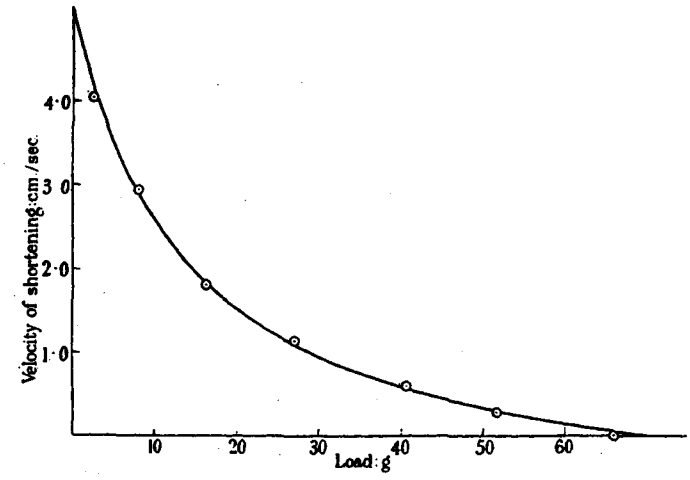

Figure 3-3 Force-Velocity Relationship (Hill, 1938)

Hill's observation that muscle force decreases with increased contraction velocity can also be explained by the sliding filament theory. Cross-bridges form and release in a cyclic pattern which results from the rate modulation of MU firings. The faster a muscle contracts, the fewer cross-bridges can be formed in any given time thus reducing force production capacity as shown in Figure 3-3. The maximum number of cross-bridges can be formed when the muscle length remains constant. Figure 3-3 refers to concentric (shortening) contractions only. Eccentric (lengthening) contractions would produce a different force-velocity curve.

Angle of Muscle Attachment

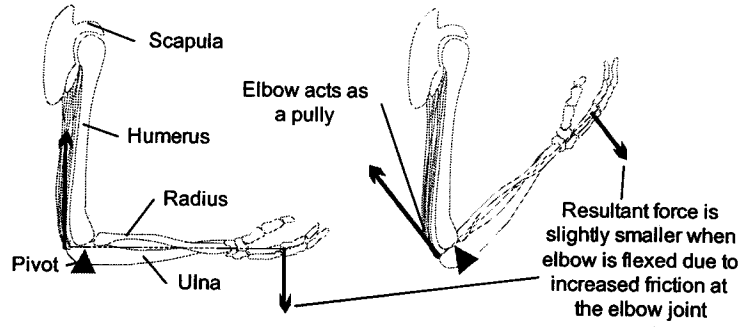

Figure 3-4 The Effect of Muscle Angle Attachment

The triceps have two points of origin on the scapula and one on the humerus. Muscle tension is transferred via tendon to the ulna directly at the point of insertion which is posterior to the elbow joint.

The elbow acts as a pulley and thus faithfully transmits the force of triceps contraction to the ulna throughout the range of motion. Torque is slightly reduced however due to an increase in friction with greater degree of elbow flexion as shown in Figure 3-4.

As the muscle contracts, some of the force developed by the contractile elements in the muscle are absorbed by the passive elastic nature of tendons and connective tissue. The time for this 'slack' to be taken up also depends on the angle of limb extension.

EMG in Dynamic Contractions

In recent years, a significant effort has been made to standardize the use of surface electromyography and to set reasonable expectations for using the technique (De Luca 1997). Even when adhering to these standards, it is understood that quantitative relationships between EMG and force can only be expected in isometric, non-fatiguing situations. Electrode placement, MU territories, and crosstalk are all factors during isometric experiments. As well, the inhomogeneous and anisotropic properties of muscle and other tissues affect the resulting electrical field. During dynamic contractions however, these issues become critically important.

When a muscle contracts dynamically, its mass shifts with respect to recording electrodes and presents a different pool of motor units to the detection field. In addition, a change in fiber orientation, interference from connective tissue, and overall altered signal conduction, all contribute to changes in the recording environment. As such, measurements made during the entire contraction cycle cannot be quantitatively compared.

Due primarily to the inhomogeneous nature of muscle tissue, it is difficult to compare muscle activation estimates for a muscle in different positions relative to the recording electrodes. The problems that arise from recording EMG in dynamic contractions are similar to those with static contraction when the electrode placement is changed. However, instead of moving the electrodes to different positions on the skin, the muscle moves relative to stationary electrodes. The net effect is similar because

EMG signals differ drastically when taken from different regions of the muscle relative to innervation and tendon zones (Masuda, Miyano and Sadoyama, 1983).

Only when all the variables in EMG recordings are taken into account can reasonable interpretations be made about the level of muscle interactions and hence force production during dynamic activities.

Dynamic Muscle Models

The majority of modern dynamic models are based on Hill's ideas of 1938. Hof and Van den Berg proposed an electrical analogue to this model. In their study, surface EMG from soleus and gastrocnemius was band-pass filtered, rectified, smoothed, and used as a quantitative measure of muscle activation. Force-length and force-velocity components were modeled using ankle angle as the input. Hof and Van den Berg assumed in their study that muscle length was proportional to joint angle. Series elastic and parallel elastic components were also taken into account. All told, thirteen parameters were adjusted and calibrated (Hof and Van den Berg 1981).

Sherif et al. noticed deficiencies in the Hof model, including the assumption that muscle length was proportional to joint angle, as well as a failure to account for electromechanical delay. They designed experiments whereby in-vivo forces produced by cat hind limb extension muscles were measured during locomotion. Their analyses lead them to suggest that EMG was best analyzed as two distinct bursts. Each burst, they suggested, corresponds to different physical manifestations of muscle contractions and should be modeled differently (Sherif et al. 1983)

Olney and Winter used a model in which subjects performed isometric contractions to calibrate parameter values for a force-EMG model. This model was then applied to walking tests by proportionately modifying the isometric relationship for muscles of different length (Olney and Winter 1985).

Traditional muscle models are relatively simple. The intention has been to maximize confidence in derived conclusions by minimizing conflicting variables. The limitation however is that such models are constrained to very specific conditions and applications. The ambition of modern biomechanics is to generalize such models. The only way to do so is to allow greater degrees of freedom. This however, significantly increases the complexity of the model. The growing overabundance of computer analysis tools can make this a slippery slope. Each additional model parameter creates numerous interdependencies within the model itself. If confidence is to be maintained in derived conclusions, each level of complexity must be met in equal measure with tighter constraints on calibrated model variables. This very struggle was experienced in the study described in the following chapter.

CHAPTER 4
SOFTWARE DEVELOPMENT

This software tool was developed to process and facilitate the biomechanical analysis of data recorded during a particular elbow extension experiment. The study involved 33 subjects, each following 17 experimental tests. The protocols consisted of concentric elbow extensions or flexions done either passively, by stimulation, isometrically, or dynamically. Five channels of data were recorded: two measuring force, two EMG and one joint angle. In total, the experimentation yielded 2805 files, each of which contained 4000 data points. Analysis required extensive processing and calculation including determining the moment of inertia, predicting force from EMG, and deriving Hill-type muscle models.

There was no software commercially available that could handle this type of data in a sufficiently meaningful way, and certainly none capable of such intense customized processing. The experimenter's original intention was to use and expand upon available analysis tools which were written in BASIC. Though these were capable of some data plotting, the majority of visual display, as well as a great degree of analysis was to be done using a spreadsheet such as Microsoft EXCEL. Needless to say, relying on these rudimentary tools would have been excessively time consuming and lead to possible processing errors. As well, they were inflexible and did not allow for easy alterations of processing protocols.

Proposed Solution

The project called for a solution that:

1. Was integrated into a single computer program.
2. Could take data from its raw state, through the entire processing protocol.
3. Allow the user to observe the effects of any modification to input parameters in order to verify each step.
4. Provide full control of process parameters.
5. Allow for easy modification of each step and if necessary, add additional processing.

The software was written in the programming Language LabVIEW by National Instruments. It seemed to be the logical choice to develop a highly customized and adaptable display and data analysis program that could meet the diverse and numerous requirements of the experiment. LabVIEW programming is done in a graphical environment that encourages modularization of code into subroutines or sub virtual instruments (subVIs) as they are called. Coding can be best described as drawing large block diagrams. Connections or wires between the blocks indicate data flow. Several examples of LabVIEW code for this software can be found in the Appendix.

The development process went beyond meeting design specifications; it required extensive collaboration with the lead experimenter. During development and testing, preliminary specifications were altered and expanded as unforeseen questions arose during each step of processing.

In this chapter, the software is described in general terms. The discussion is not specific to programming language. In fact, only generalized overviews of the algorithm are presented. Flow charts are used to illustrate data flow and processing. Though a

significant part of the program is devoted to user friendliness and functionality, explanations for these are kept simple wherever possible. Firstly, such aspects cannot be described without heavy reliance on the LabVIEW programming environment, and secondly, they are of lesser importance than those directly related to the physiology and biomechanical problems at hand.

Measurement System

The goal of the biomechanics study was to explore the mechanisms involved in athletic ballistic activities such as jumping or throwing. If the project could be reduced to answering one question it would be "What is the nature of the relationship between a muscle's maximum strength and its maximum speed of contraction?"

Jumping for example, is a very complex task with numerous interdependencies such as multiple joint actions, multiple muscle activities as well as more complex factors such as muscle coordination and central motor drive. A simple ballistic task was chosen to isolate the dynamics of a single muscle: the triceps of the upper arm.

Subjects performed forearm extensions. They did so at maximal effort and against varying resistances. Their forearms were strapped to a device shown in Figure 4-1 which ensured movement in a single plane. Extensions were performed from an angle of approximately 90° to full extension.

For each of the 33 subjects, 5 channels of data were recorded as shown in Figure 4-2. These were triceps and biceps EMG, forearm force, torque and joint angle. As stated before, each subject performed 17 tasks: passive slow movement of the forearm, passive

fast movement of the forearm, a stimulated twitch contraction, a post activation twitch contraction, maximum effort isometric extensions at 60°, 90°, and 120° joint angles, maximum effort isometric flexions at 60°, 90°, and 120° joint angles, dynamic extensions at 20%, 40%, 60% and 80% maximum effort, dynamic extensions at 11 N and 2.2 N of force, and a fatigue trial.

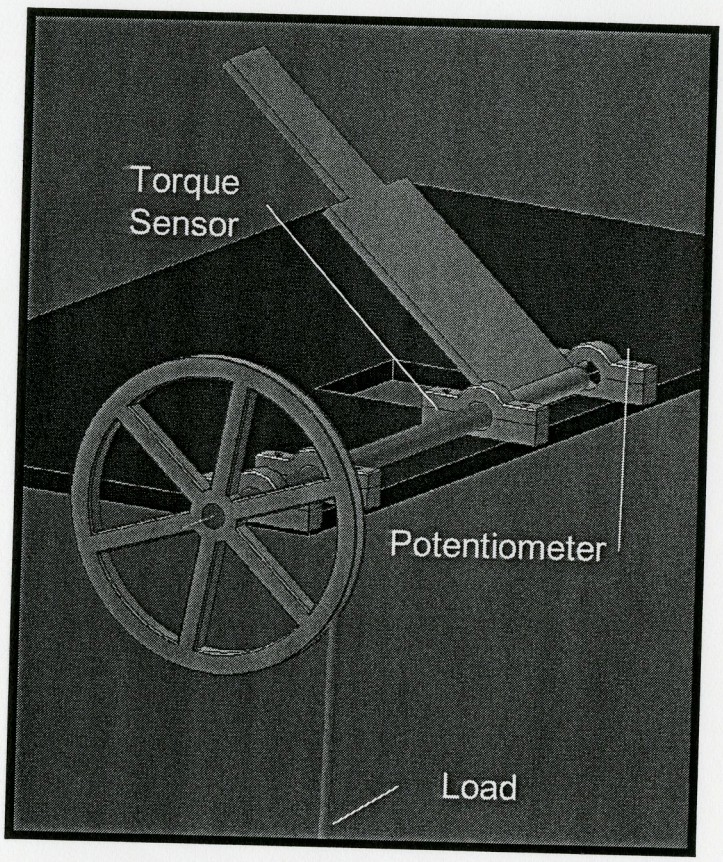

Figure 4-1 Elbow Extension Apparatus

Resistance was varied by changing the weight lifted by the wheel in Figure 4-1. A sensor was attached to the wheel connecting rod to measure torque produced during

experiments. The apparatus was also used for isometric trials whereby the forearm was held at a constant angle of extension. A separate load sensor was used to measure force. There was a third sensor located at the rod pivot point to record angle of extension.

Data Measurement and Recording

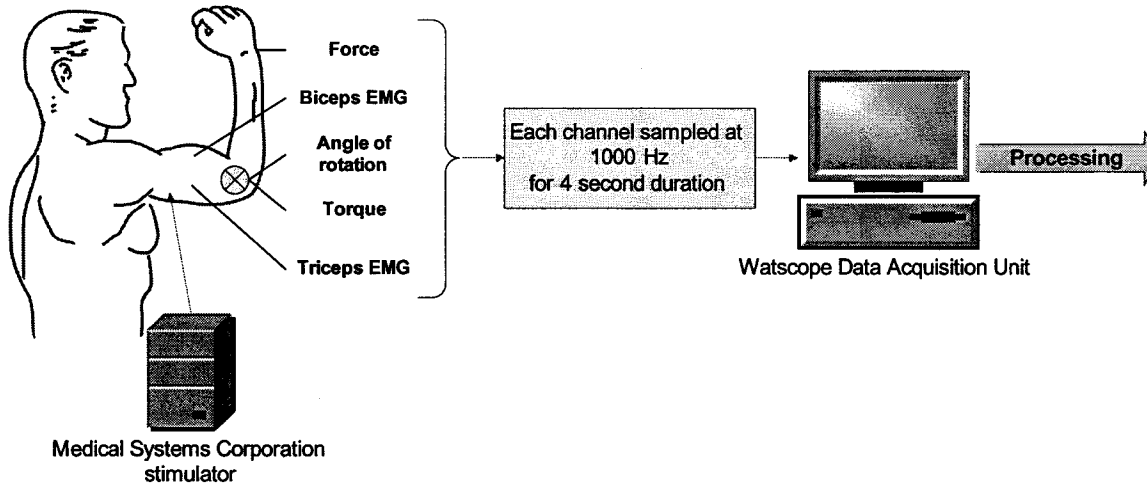

Figure 4-2 Data Acquisition and Storage

Surface EMG was measured from triceps and biceps muscles using Delsys bipolar dry surface electrodes attached to the skin. The signal was amplified using custom built EMG amplifiers. Triceps were stimulated to evoke twitches using a constant voltage stimulator by Medical Systems Corporation. Fatigue trials were done on a Cybex II isokinetic dynamometer made by Lumex Incorporated.

As show in Figure 4-2, a Watscope Data Acquisition Unit by Northern Digital Incorporated, recorded data from the load cell, torque sensor, potentiometer and from the EMG amplifiers. All signals were sampled at 1000 Hz for durations of 4 seconds, except for the fatigue trials which were recorded for durations of 80 seconds. The sampling frequency was sufficiently high to accommodate the bandwidth of surface EMG. All experimental data was saved to hard disk for subsequent processing.

Project Objective

The objective of the project was to build an EMG driven model of triceps contraction. A series of experiments were designed by the experimenter to calculate the value of parameters which when applied to triceps EMG could accurately predict muscle force in a dynamic contraction.

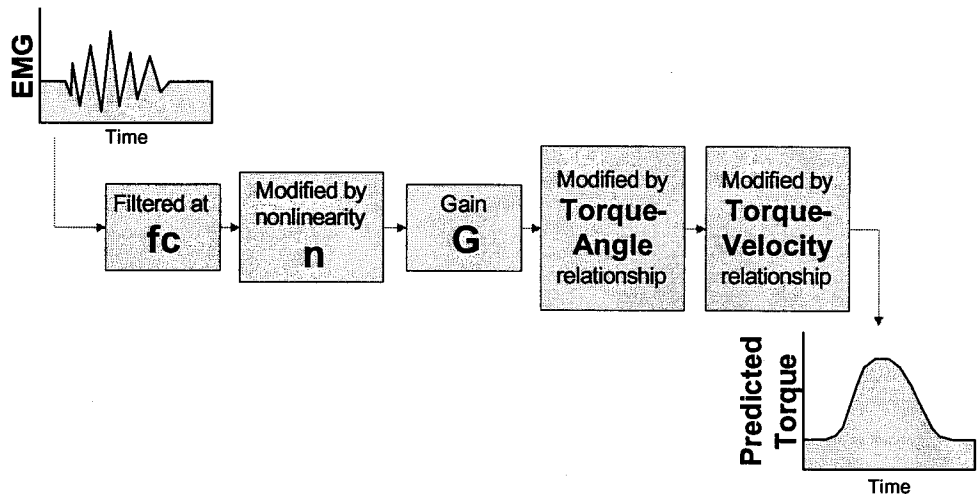

Figure 4-3 Torque Predicting Model and Associated Parameters

The parameters of the model are: the EMG linear envelope cutoff frequency (*fc*), a nonlinearity factor (*n*), gain (*G*), the torque-angle relationship, and the torque-velocity relationship. Equation 4-1 shows the model parameter equation.

$$\text{Torque} = G\,[(\text{EMG}) \text{ filtered at } fc]^N$$

Where:
fc = linear envelope cutoff
N = nonlinearity factor
G = gain

Equation 4-1 Muscle Model Equation

Torque that is predicted from this model is compared to experimentally measured torque. The model parameters are optimized to minimize the error between predicted and measured values. Once optimized, a comparison can be made between subjects exhibiting differing strength and speed. It was hoped that insight might be gained by comparing their respective parameters. Subjects with similar strength, but significantly different contraction speeds for example would be of particular interest. The expectation was to find clues to such differences within the model parameters.

The motivation for creating these models was to eventually develop a guide for improved athletic performance. Perhaps one day, training programs could be designed to improve an athlete's overall performance based on improving a particularly weak model parameter.

Program Modules

The following pages show the module user interface panels followed by a description of how they work. Of primary importance was ease of customization of input

parameters. The goal was to be able to change an input and instantaneously see the result of that change on processed data.

Plot and Process Module

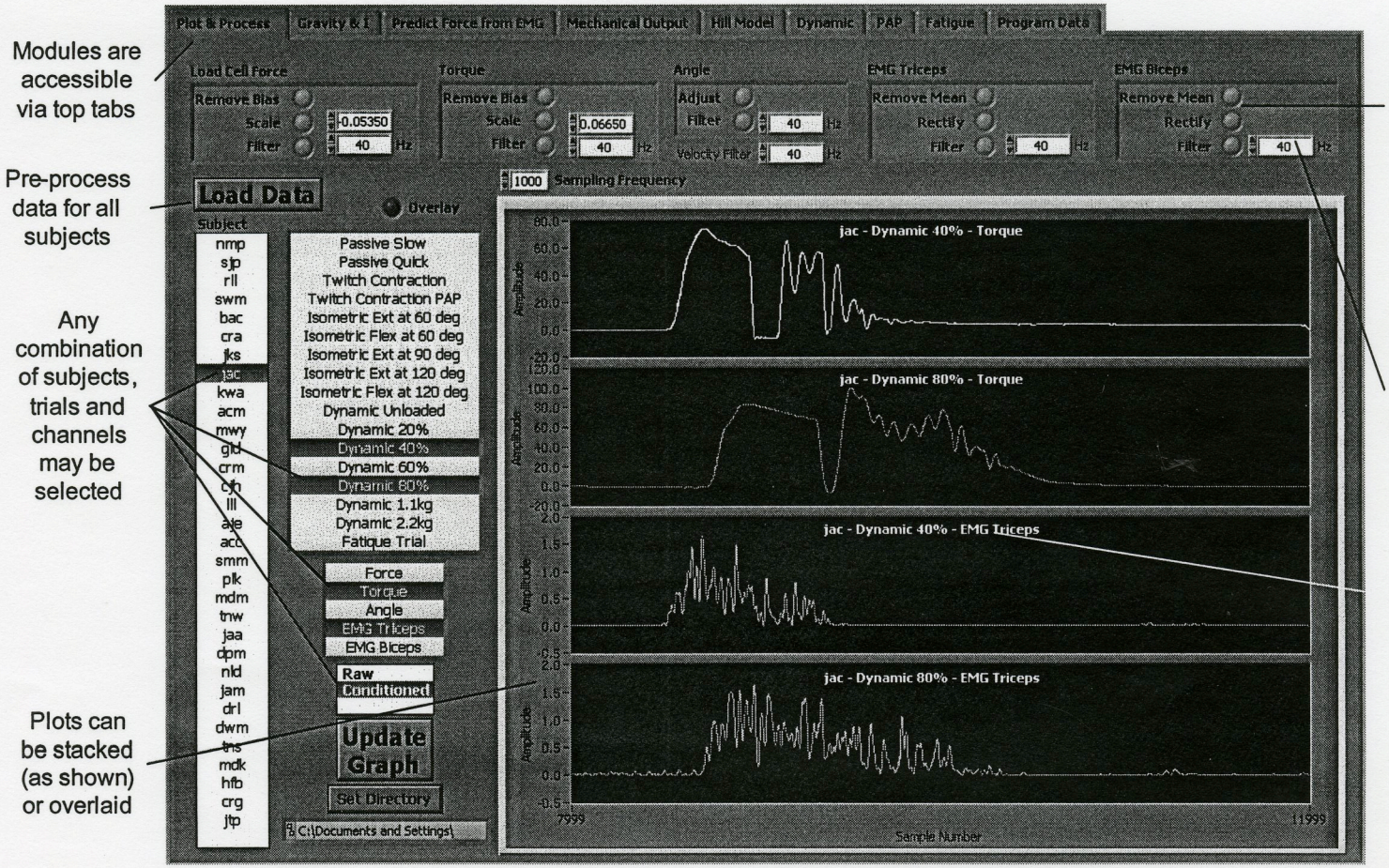

Modules are accessible via top tabs

Pre-process data for all subjects

Any combination of subjects, trials and channels may be selected

Plots can be stacked (as shown) or overlaid

Each step of the processing can be turned on or off

Values for each processing step can be adjusted

Plots are automatically labeled

Figure 4-4 Plot and Process User Interface Panel

The first problem was how to manage and selectively display 2,805 files worth of data. A module was developed by which the user can choose any combination of subjects, protocols and channels with the click of a mouse and display the associated data either on separate stacked graphs as shown in Figure 4-4, or have them superimposed. This figure shows the torque and triceps EMG data recordef for 40% and 80% maximum effort extensions of subject jac.

In addition to 'raw' data, some basic processing is done on each channel before it is used by the rest of the program. This "pre-processing" is incorporated into the plotting page so that the effects of each step such as gain and filter cutoff setting can be visualized and adjusted by the user. Furthermore, the user has the choice to skip any processing step as shown in Figure 4-5.

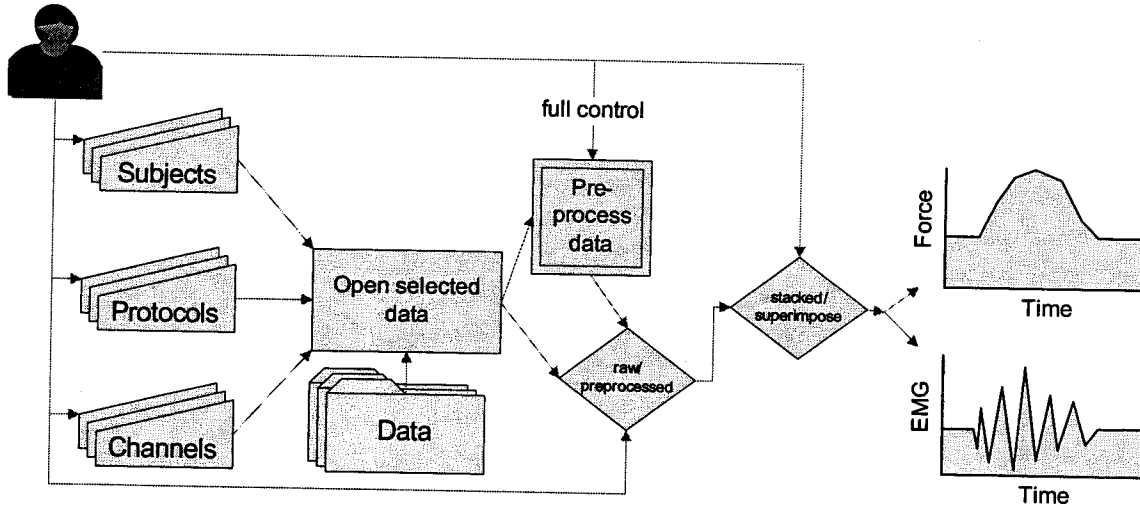

Figure 4-5 Plot User Selected Data

The load cell and torque signals are processed as shown in Figure 4-6. In order to 'zero' the signals, the first 100 data points are averaged to determine the offset for load cell and torque meter. This bias is then removed from all data points. The next step is to scale the signal so that numerical data point values correspond to actual Newtons and Newton Meters respectively. Finally, the data is filtered to remove high frequency noise. Typical lowpass cutoff frequency chosen was 40 Hz as shown in Figure 4-4. This value was chosen to avoid band limiting the signal while removing the dominant 60 Hz noise.

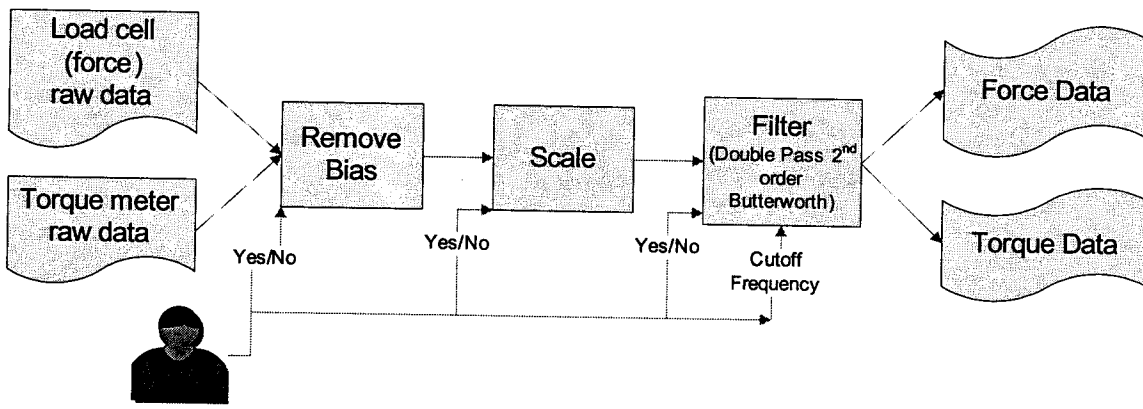

Figure 4-6 Load Cell and Torque Meter Signal Processing

For each subject, the apparatus was calibrated for rotation angle by recording the potentiometer signal at 60° and 90° as shown in Figure 4-7. These angles were measured from the point of maximum elbow flexion which was taken to be 0°. A linear fit is done on the calibration data in order to derive an accurate angle of rotation. Velocity of rotation is calculated by differentiating the angular position with respect to time via a difference of adjacent samples. Both angle and velocity data is filtered to remove high frequency noise. Typical lowpass cutoff frequency chosen was 40 Hz.

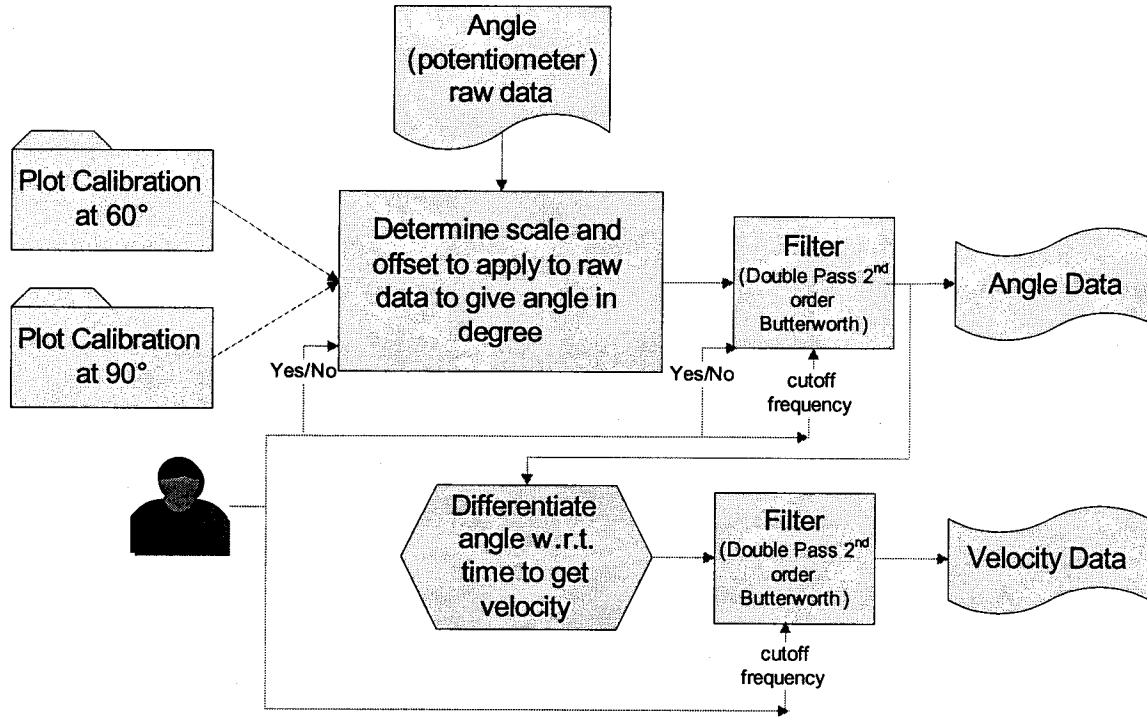

Figure 4-7 Angle Calibration and Preprocessing

EMG from triceps and biceps muscles are subjected to the most common EMG transforms: removing of bias, full wave rectification, and filtering.

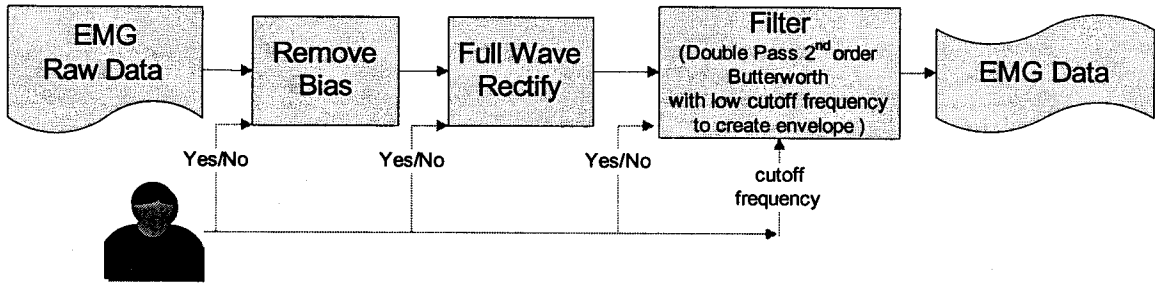

Figure 4-8 EMG Preprocessing

The user can use the 'Process and Plot' page for quick access to any one data file, or to compare files between subjects. For example, a user can plot the torque and elbow angle from two different subjects during isometric extension at 90° and 120° simply by selecting the desired 'subjects', 'protocols' and 'channels' from their respective input boxes and clicking the 'Update Graph' button.

The user can explore the effect of changing the cutoff frequency of filtered EMG data and observe the resulting linear envelope with the click of a button.

Finally, before proceeding with the rest of the program, the user chooses one subject whose data will be made available for all subsequent analyses.

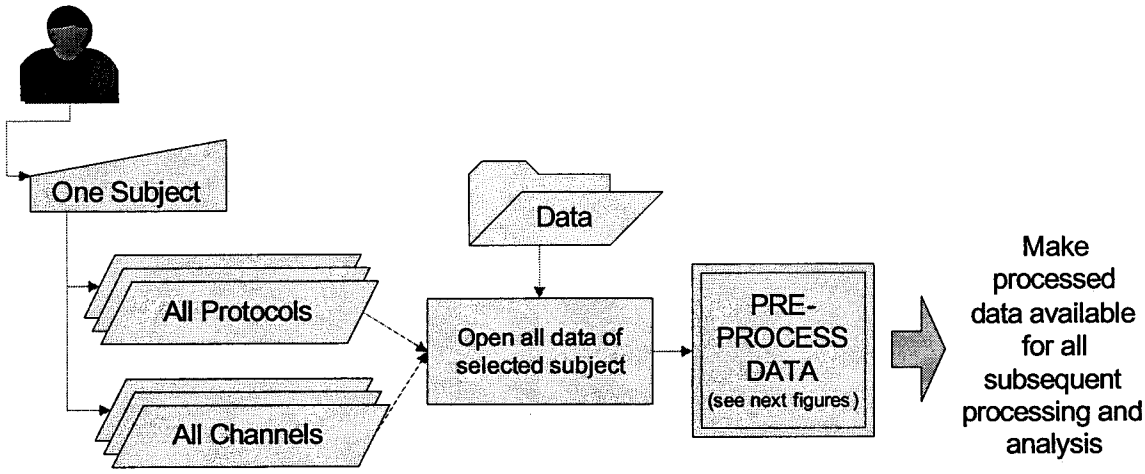

Figure 4-9 Process all Data from Selected Subject

Gravity and Moment of Inertia Module

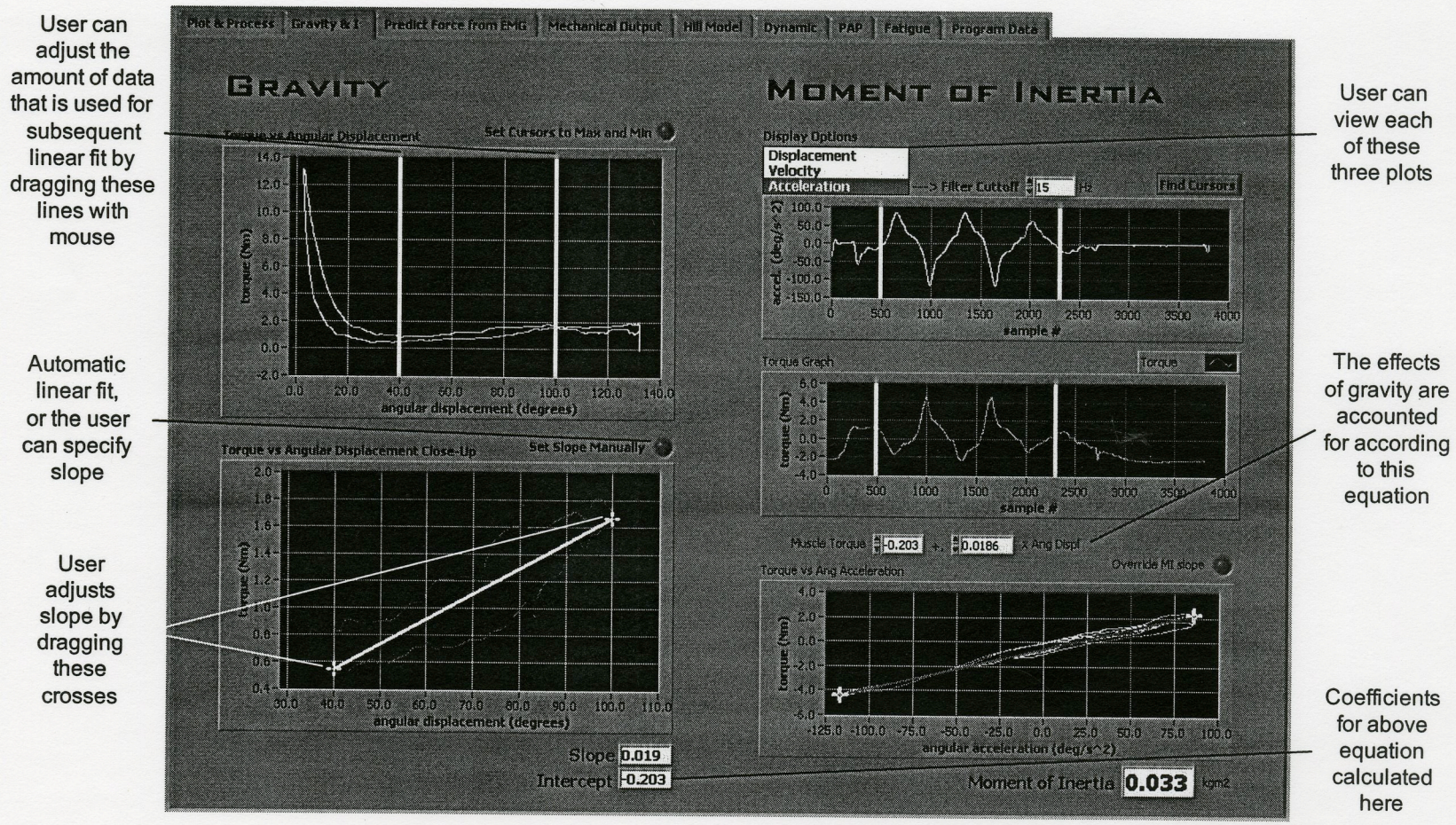

Figure 4-10 Gravity and Moment of Inertia User Interface Panel

The effects of gravity on the apparatus as well as the moment of inertia of the forearm and apparatus level arm are calculated in order to determine the true torque produced by the triceps. Equation 4-2 shows the calculation for true muscle torque.

$$Tm = Ts - Tg(\theta) - I \cdot \alpha$$

Where:

Tm	=	muscle torque
Ts	=	measured torque
Tg(θ)	=	torque caused by gravity on forearm and lever arm as a function of extension angle
I	=	moment of inertia of forearm and apparatus lever arm
α	=	angular acceleration of extension

Equation 4-2 True Muscle Torque Equation

Gravity and Passive Moment Module Description

The weight of the forearm and apparatus lever register a torque even when the subject is at rest. This torque is different depending on the system's vertical component of force due to gravity. This component is dependent on extension angle. The first trial involved slowly rotating the wheel and passively taking the resting subject through the range of elbow extension. The subject's forearm is moved from maximum flexion (0°) where there is considerable resistance due to tissue compression resulting in high torque values, to maximum allowable extension. The resulting torque is plotted versus angular displacement as shown in Figure 4-10. The first and last quarter of data is unusable because of soft tissue compression at flexion and because the apparatus would hit the table at maximum extension. Only the middle half of the data is used to determine a

linear approximation as outlined in Figure 4-11. Although the relationship is a function of sine of (joint angle - 40°), considering noise and experimental error, a linear approximation is reasonable.

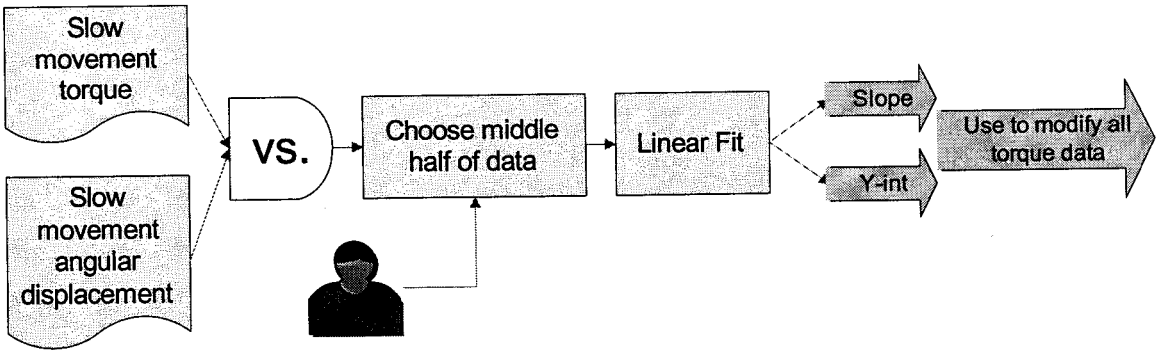

Figure 4-11 Compensating for the Effects of Gravity

Moment of Inertia Module Description

The next experimental protocol moves the subject through the entire range of motion several times, but this time quickly enough to cause measurable acceleration. Acceleration is calculated by differentiating the velocity with respect to time. Velocity is calculated by differentiating angular displacement. Data is filtered to reduce measurement noise which is enhanced by each differentiation. Typical cutoff frequency chosen was 15 Hz. Torque is then plotted versus angular acceleration from data again selected by the user as shown in the right half of Figure 4-10. The slope of this line is the Moment of Inertia of the forearm and associated apparatus since torque is the product of Moment of Inertia and angular acceleration.

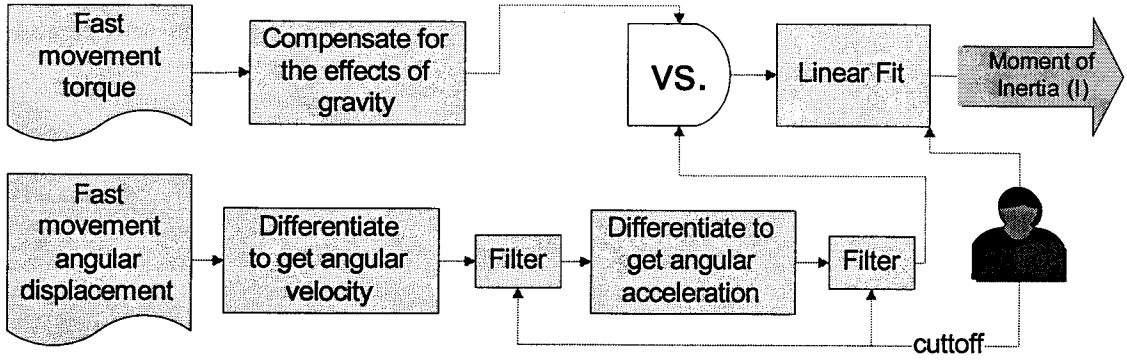

Figure 4-12 Calculating the Moment of Inertia

Mechanical Analysis Module

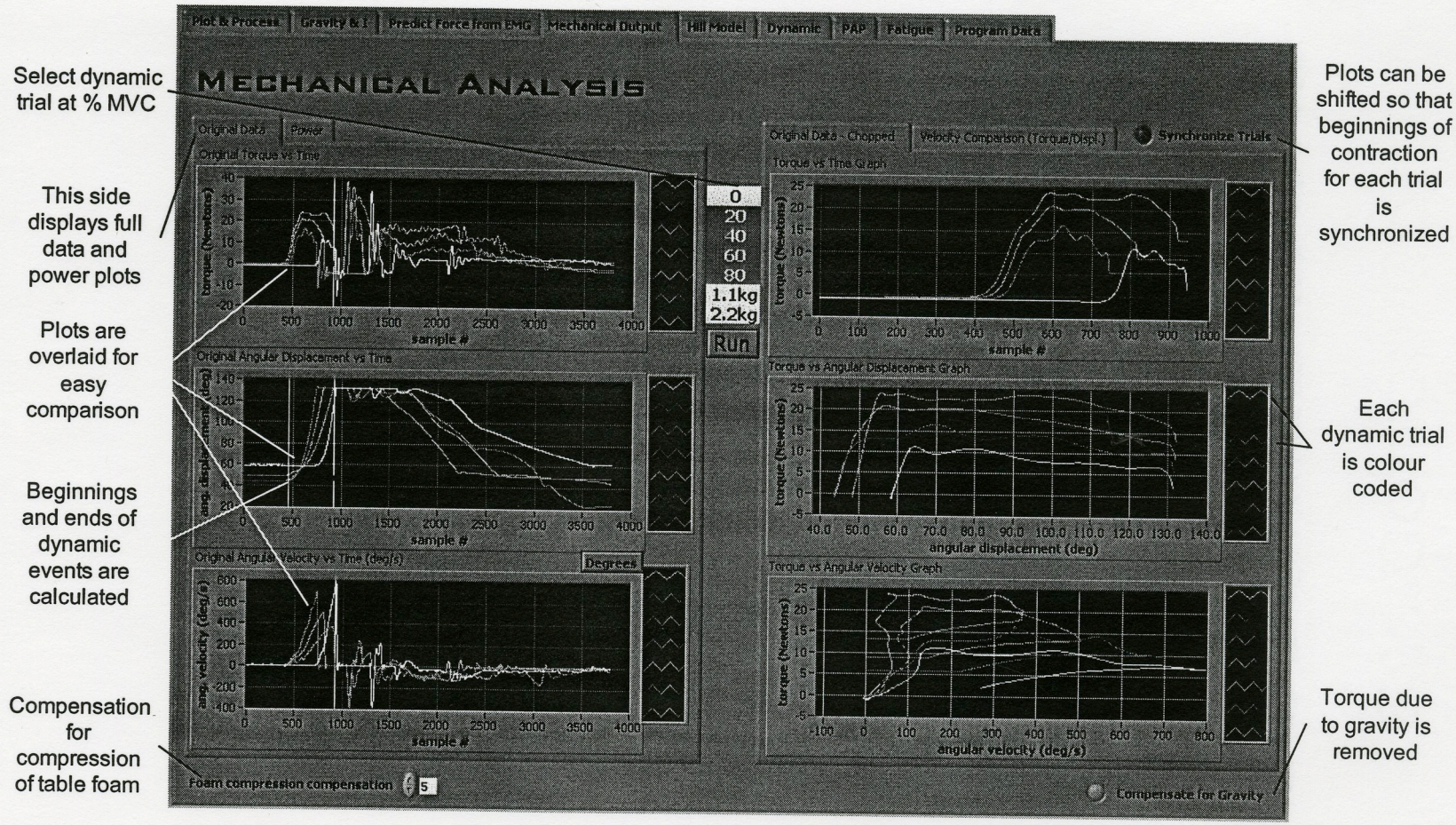

Figure 4-13 Mechanical Analysis User Interface Panel

The purpose of this module is to plot and analyze the mechanical data of the dynamic trials. In these experiments, subjects performed single elbow extension against a resistance normalized to a percentage of subject Maximum Voluntary Contraction (MVC). Seven different resistances were used from 0% to 80% MVC. The following data is plotted for as many trials as the user selects as shown in Figure 4-13:

- Torque vs. Time
- Angular Displacement vs. Time
- Angular Velocity vs. Time

Next, the power is calculated for each trial and the following plots made:

- Power vs. Time
- Power vs. Angular Displacement
- Power vs. Velocity

Power was calculated as the product of torque and velocity. Plots proved not to be as useful, hence not shown in Figure 4-13.

Finally, the program automatically determines the beginning and end of the extension motions. The beginning point is determined from the angular displacement data when the subject rotates forearm by one degree beyond rest position. The end point is determined where velocity becomes zero as the result of hitting the table. The data beyond end of motion is discarded and the following plots made as shown on the right side of Figure 4-13.

- Torque vs. Time
- Torque vs. Angular Displacement
- Torque vs. Angular Velocity

Figure 4-14 summarizes the process to determine the mechanical variables for the trials.

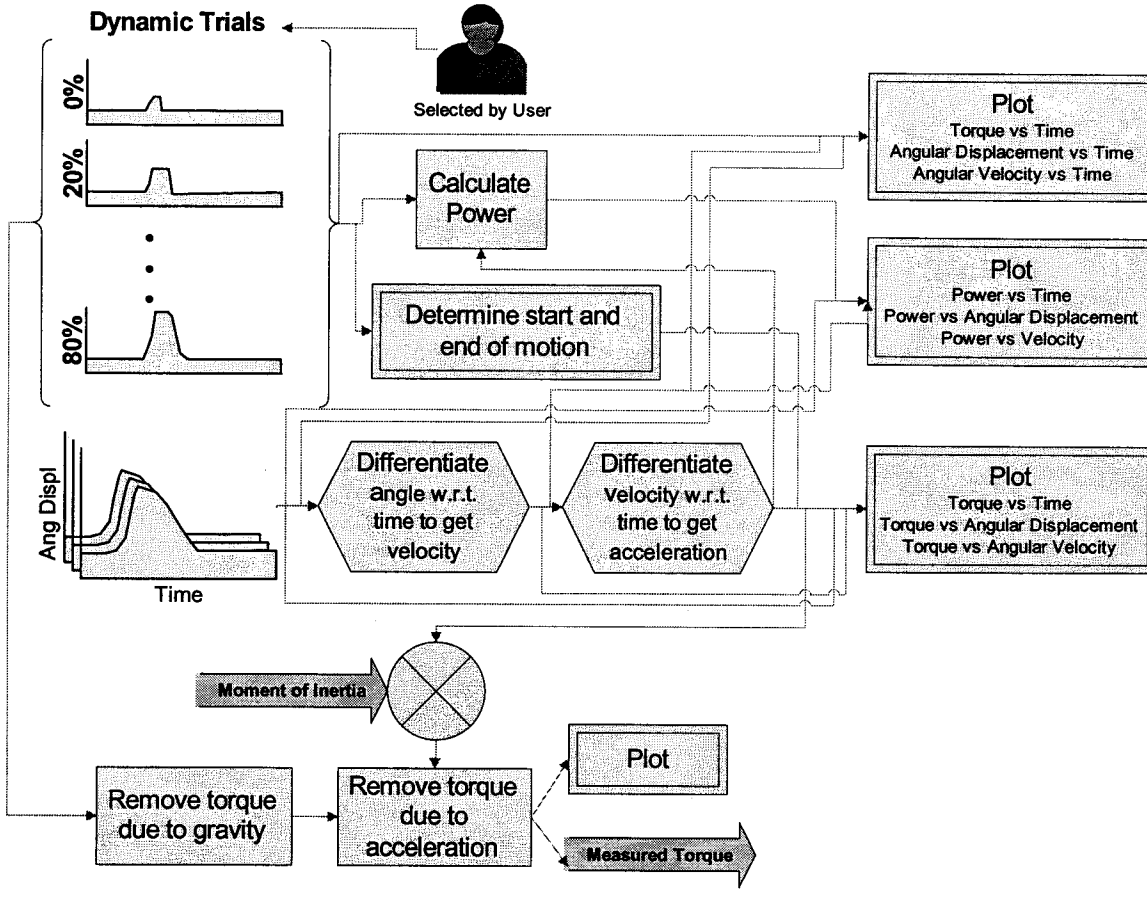

Figure 4-14 Mechanical Output Module Overview

Finally, the actual muscle torque is calculated by subtracting the effects of gravity and force due to accelerating the forearm and apparatus from the measured values of torque as shown in Figure 4-14.

Predict Force from EMG in Static Contractions Module

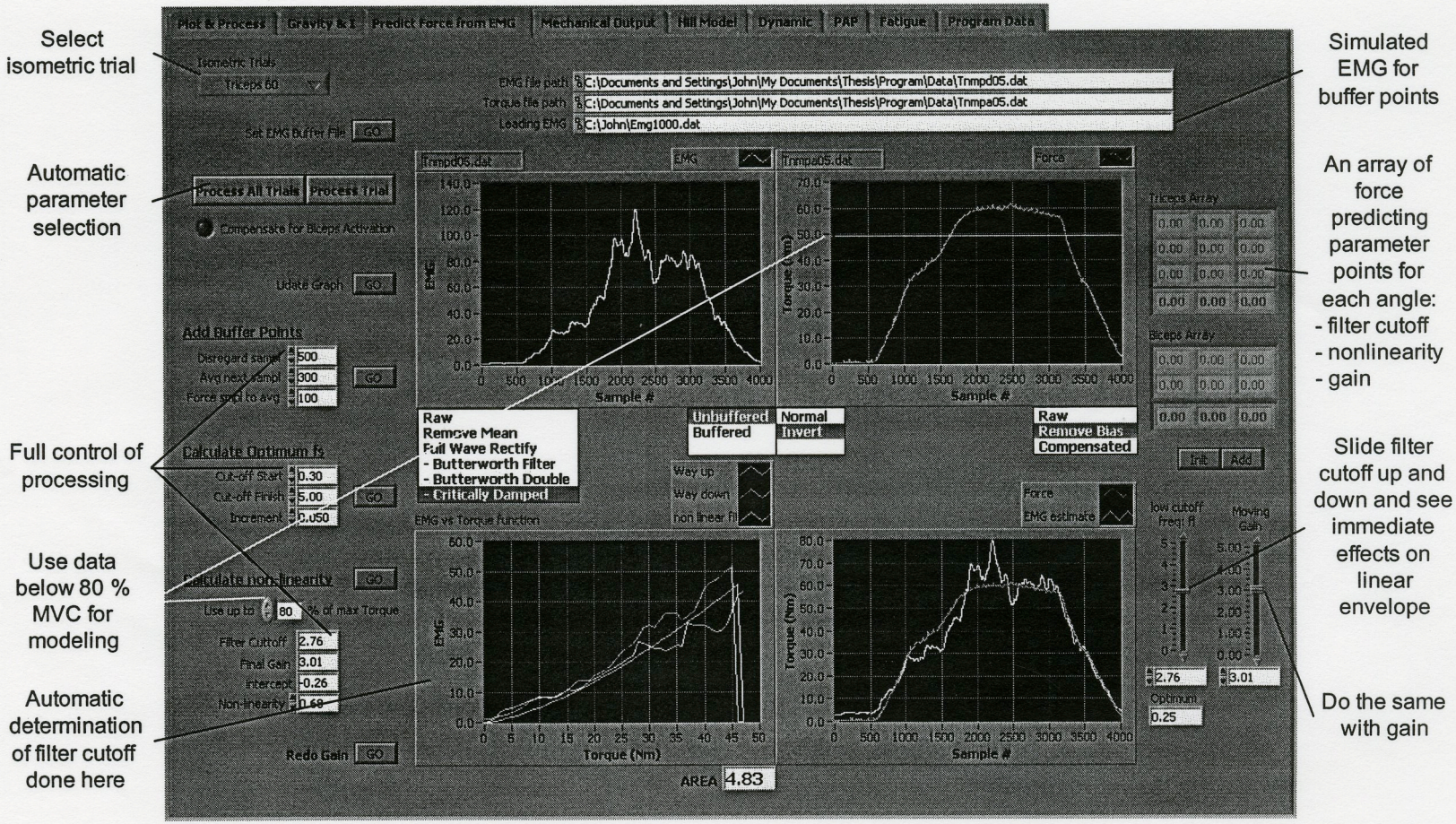

Figure 4-15 Predict Force from EMG User Interface Panel

In order to predict torque from EMG in dynamic trials, analyses must first be done on the isometric experiments. A model is created to relate force and EMG in an isometric contraction. Values for the parameters that belong to such a model are recorded and then used to predict force in dynamic contractions. The variables in this case are: gain, linear envelope cutoff frequency, and a nonlinearity factor. In this case, co-contraction was minimal as shown by EMG of biceps in normal movements of the type studied here and could be ignored.

$$\text{Torque} = \mathbf{G}\,[(\text{EMG})\ \text{filtered at}\ \mathbf{fc}]^{\mathbf{N}}$$

Where:

fc = linear envelope cutoff
N = nonlinearity factor
G = gain

This module has been designed to automatically choose these variables while also allowing for manual selection and adjustments. This program loops continuously so that the user can change a setting such as cutoff for linear envelope and immediately see the result in the output displays.

The first step is to process the triceps EMG signal as shown in Figure 4-16.

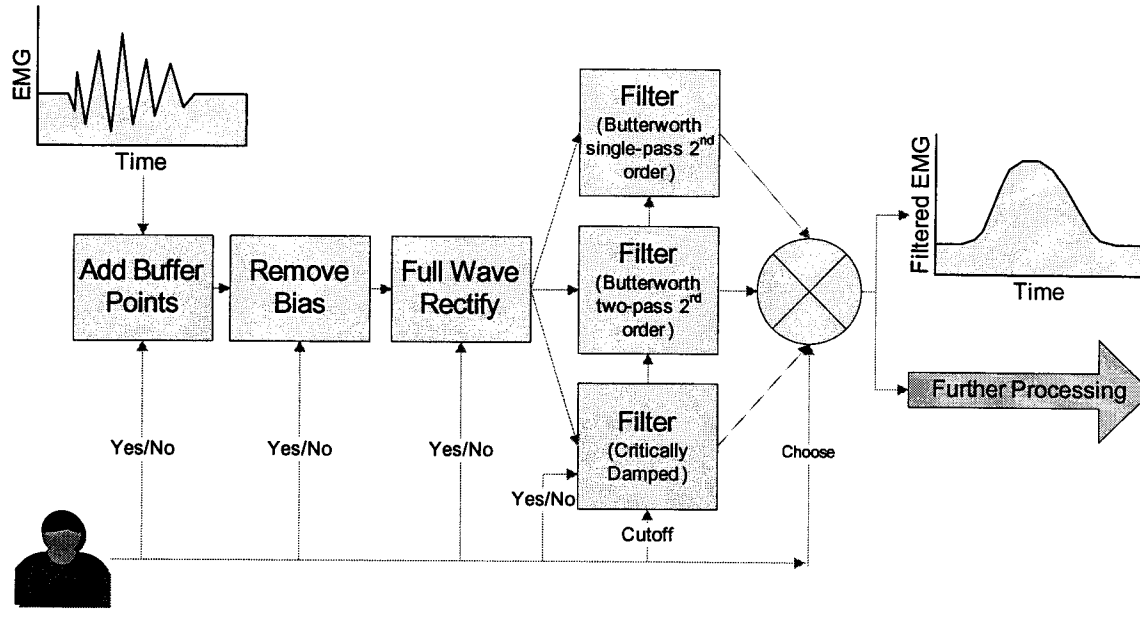

Figure 4-16 Process Triceps EMG

Buffer points are added so as to provide a smooth lead-up to initial data. Any bias that may be present in the signal is removed by subtracting the average of the first 100 data points. This raw EMG is then full wave rectified and then subjected to a low pass filter to create a linear envelope. The choice of filter is left up to the user. The two pass Butterworth and critically damped filters (Dr. J. Dowling, McMaster University) serve to minimize phase distortion due to filtering.

Next, the elbow torque data is processed as in Figure 4-17.

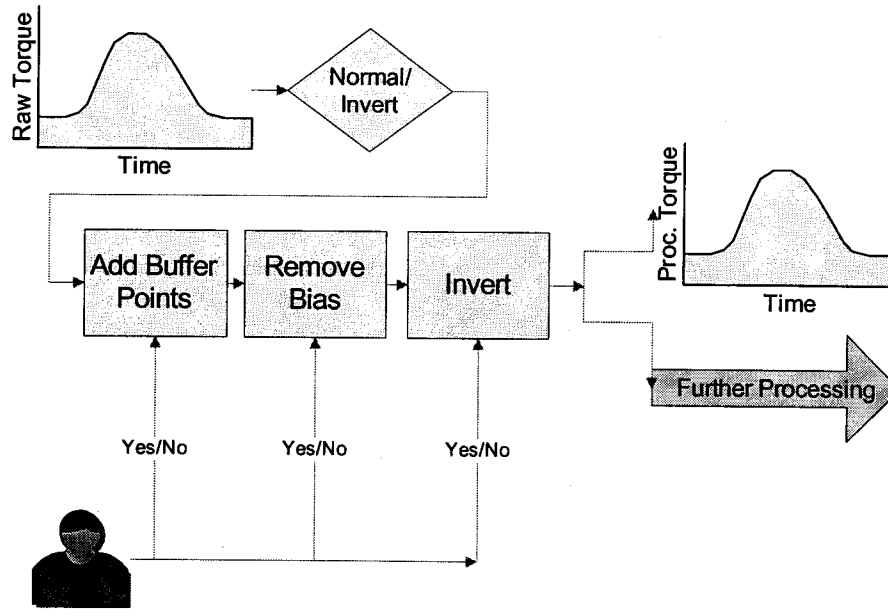

Figure 4-17 Process Elbow Torque

Buffer points are added to match those chosen for the EMG processing. The torque meter may not have been calibrated to give a zero value at rest, so any bias is removed by subtracting the average of the first 100 data points. In some cases the torque data was saved inverted, and so the user has the option of correcting for that.

The program can automatically calculate an optimum cutoff frequency for the filter used to create the linear envelope. The type of muscle contraction used for this module was a gradual increase to MVC followed by a gradual decrease to rest. When the linear envelope of the EMG is plotted versus corresponding torque, the resulting plot forms a hysteresis loop. Optimum cutoff is that which results in a minimum hysteresis area. The algorithm used is show in Figure 4-18.

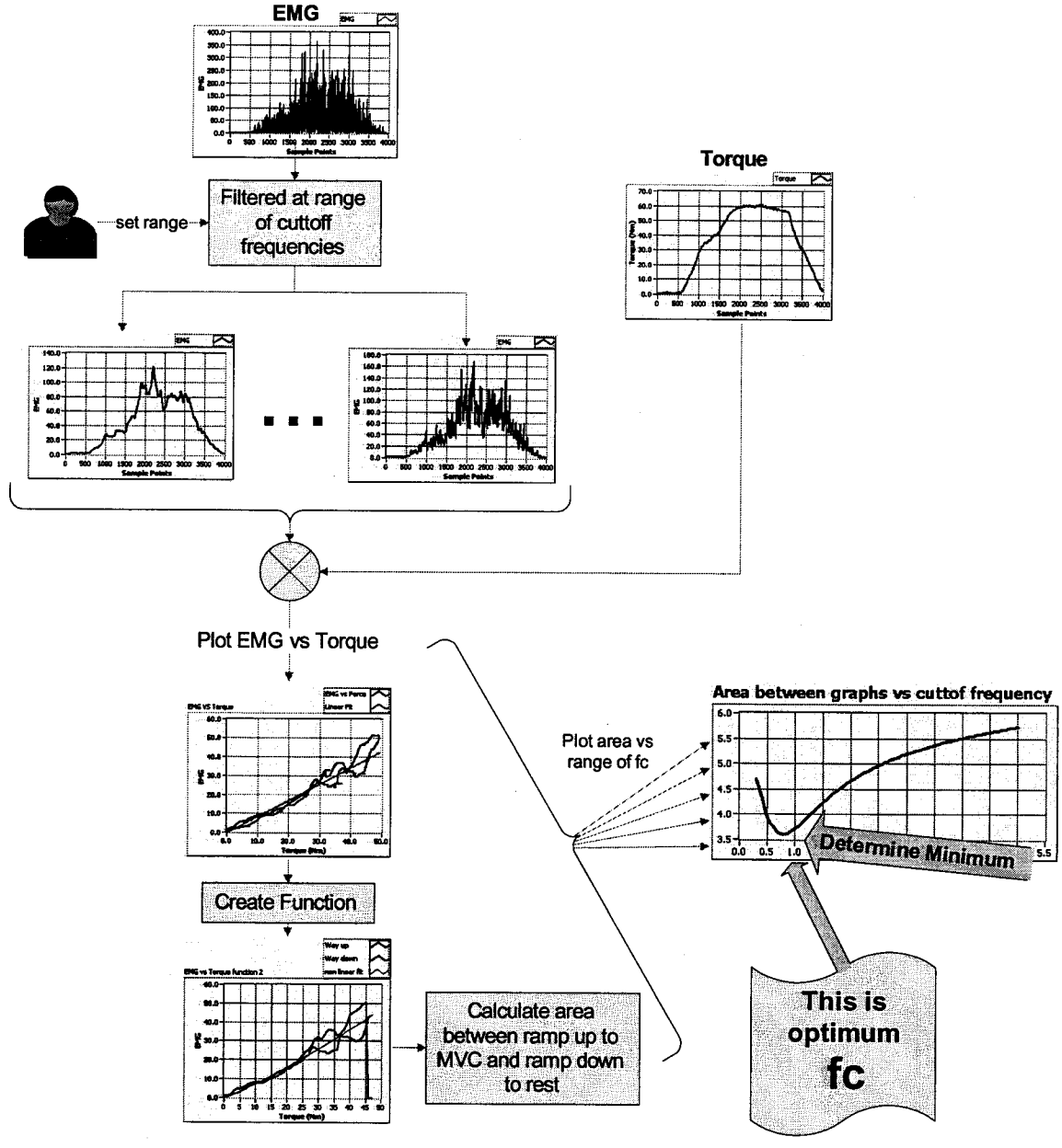

Figure 4-18 Calculating Optimum Cuttoff Frequency for Linear Envelope

The range and step interval for the cutoff frequencies is controlled by the user. After filtered EMG is plotted versus torque, the resulting waveform is converted to two functions: one corresponding to contraction up to MVC and the second from MVC to rest. This is done by first splitting the data at mid point of contraction. Then, the data points are converted into functions by accepting only one y-coordinate for each x-value. Note that placeholders must be introduced so as not to shorten the true length of the functions. This process is necessary in order to calculate the area between these two graphs. Areas are then recorded for each value of cutoff frequency in the range set earlier by the user. The minimum area corresponds to the optimum cutoff frequency (fc).

Once this cutoff is determined, the program calculates the gain (G) from the slope of the line of best fit. A linear regression analysis minimizes the deviation of data points from this linear approximation. Finally, the program determines non-linearity by minimizing the error between the data points and a line whose function is raised to the power of a non-linearity factor (N).

Automating this process removes user bias in the selection of model variables. These variables are calculated for triceps data from isometric MVC of elbow extension for elbow angles set at 60°, 90°, and 120°. The three values for each trial are averaged and then used to predict force in the dynamic experiments.

The user has the freedom to adjust any computer chosen variable. A certain amount to user subjectivity is often desired. Pure mathematical minimization considering all variables simultaneously may result in a non physiological solution.

Hill Model Module

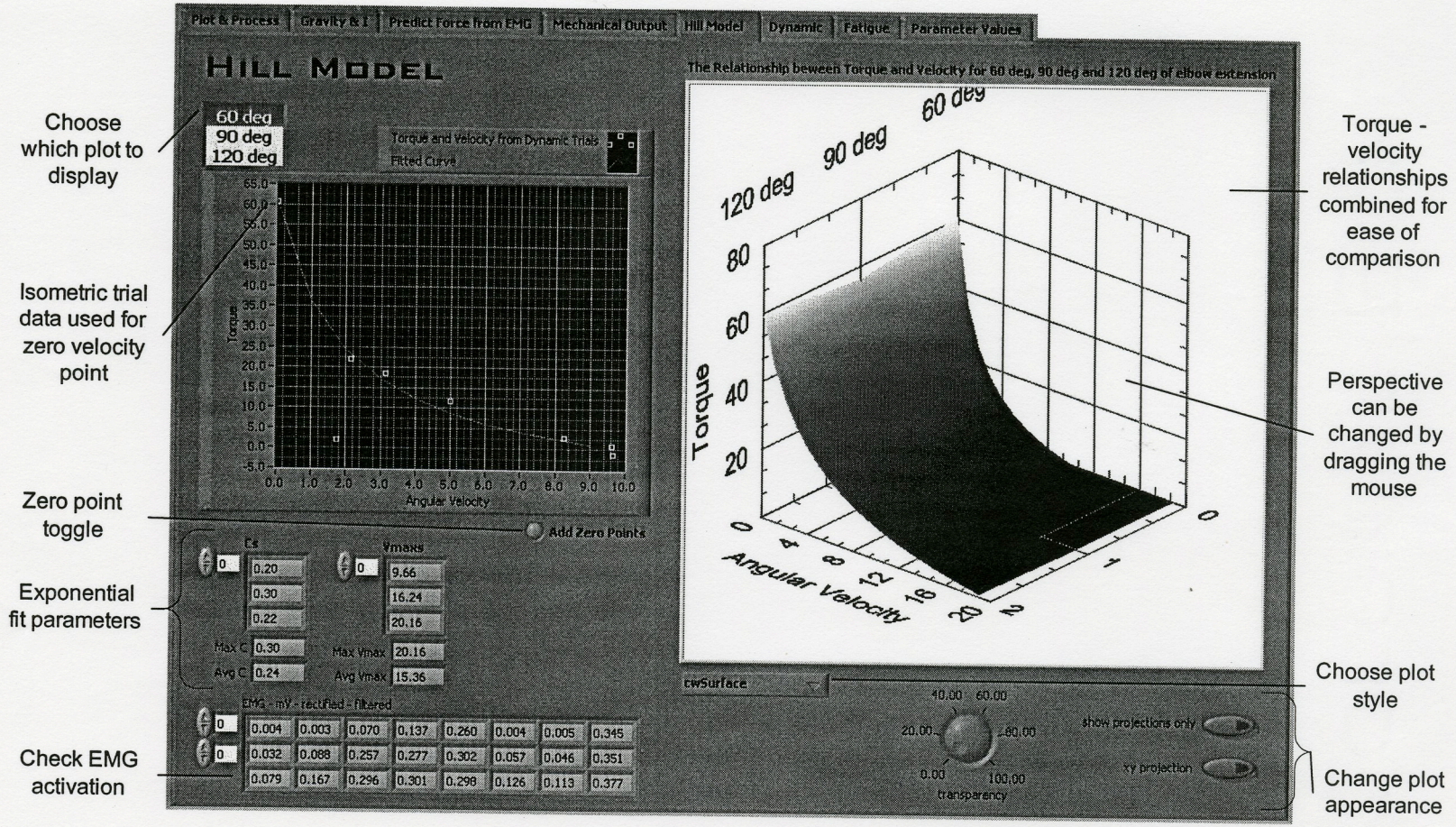

Figure 4-19 Hill Model User Interface Panel

This module derives a torque-velocity relationship of subject triceps muscles from the dynamic contractions that were already partially analyzed in the Mechanical Analysis module. Three torque-velocity curves are calculated for each subject, at elbow angles of 60°, 90°, and 120°. Angular displacement data is examined to find the time index when elbow extension crosses the 60°, 90°, and 120° marks. This is done for each dynamic trial from 0% MVC to 80% MVC. These time indices are then used to find the corresponding torque and velocity of extension rendering seven pairs of points for each of the three extension angles. An eighth pair of points is derived from isometric trials. Maximum torque is paired with a velocity of zero and added to the above seven dynamic points. The process is shown in Figure 4-20. The force velocity relationships are plotted on two dimensional graphs and combined on one three dimensional graph for easy comparison. The controls and displays available to the user are shown in Figure 4-19.

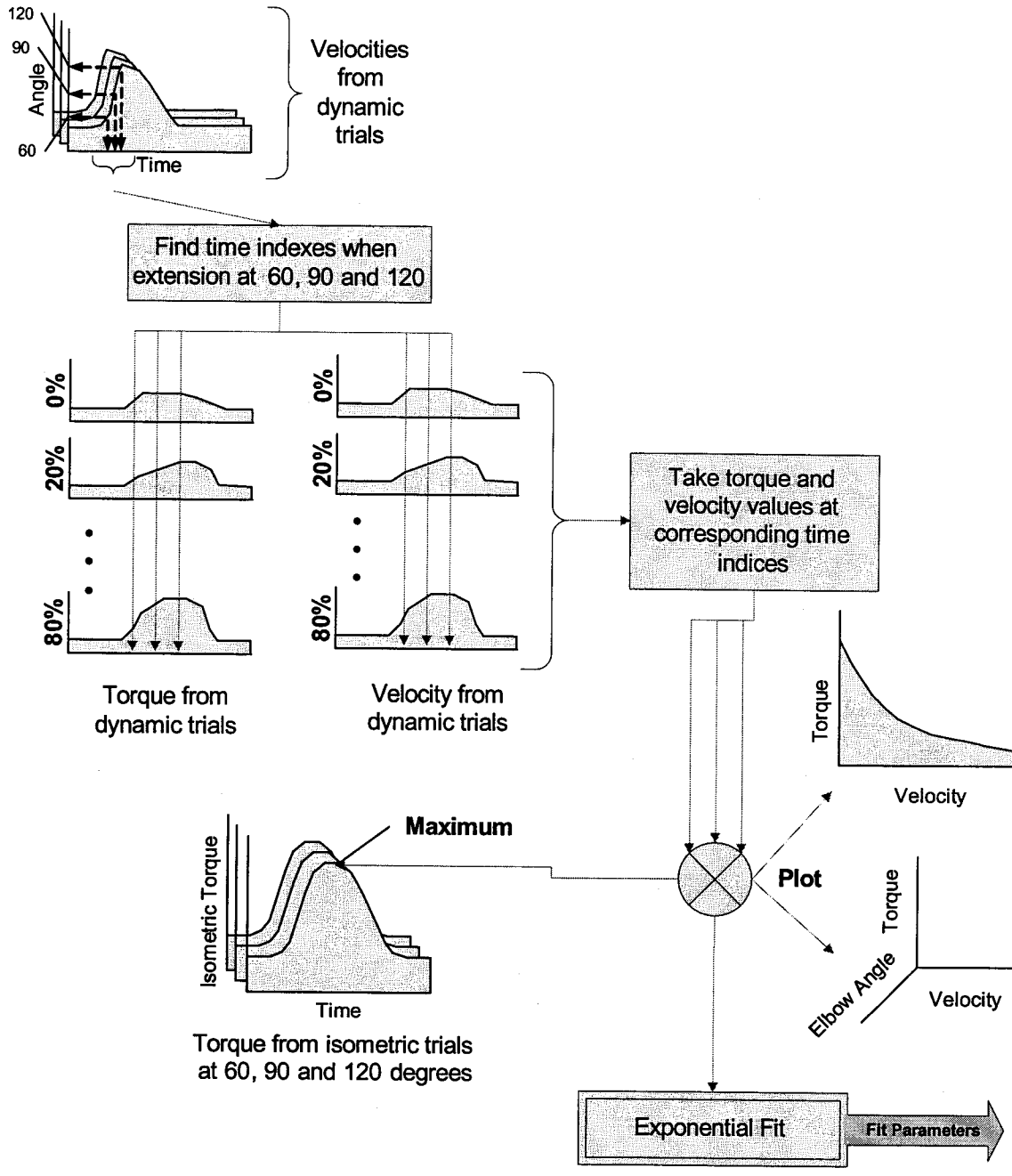

Figure 4-20 Hill Model Module Overview

Dynamic Muscle Model Module

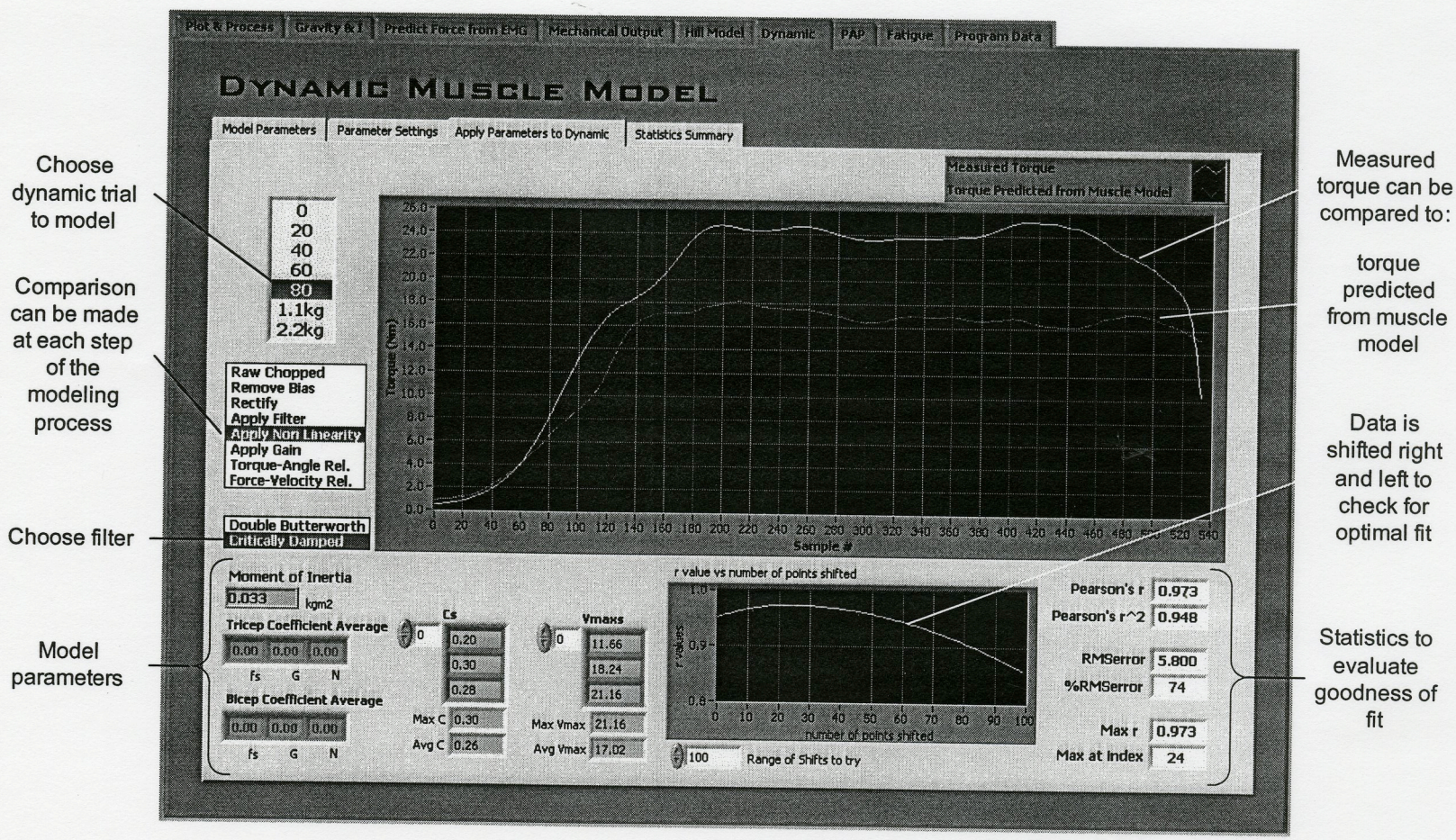

Figure 4-21 Dynamic Muscle Model User Interface Panel

This module integrates the modeling variables in Equation 4-1 derived from all the previous analyses of the isometric trials and applies them to the dynamic experiments. Dynamic EMG is rectified, filtered, raised to the exponent nonlinearity factor, amplified by a gain, and then modified by the torque-angle and force-velocity relationships. A Pearson's statistical analysis is done between predicted and measured torque and the RMS error calculated as shown in Figure 4-21.

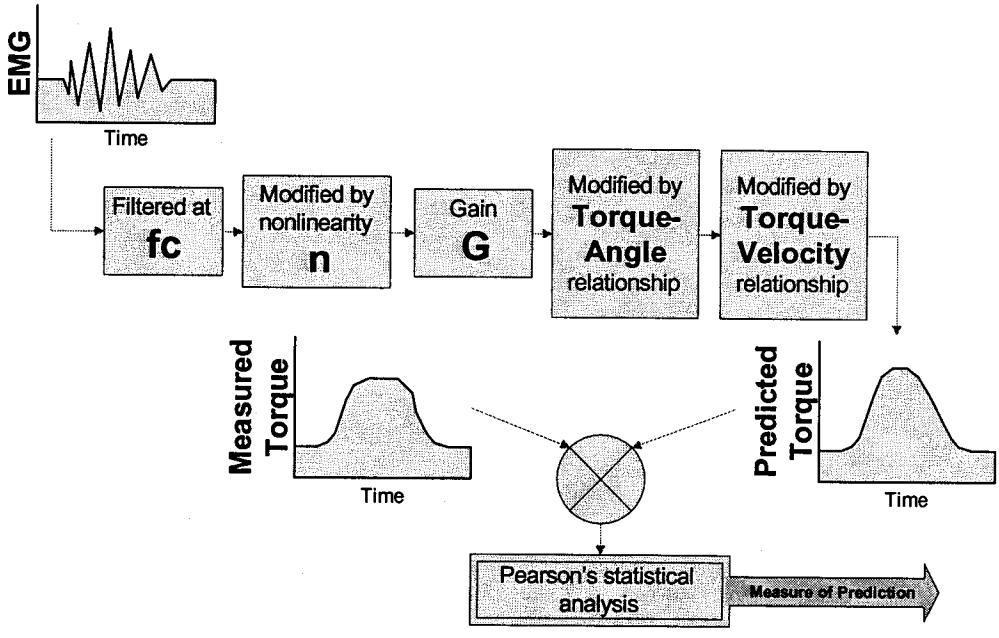

Figure 4-22 Dynamic Model Module Overview

Postactivation Potentiation Module

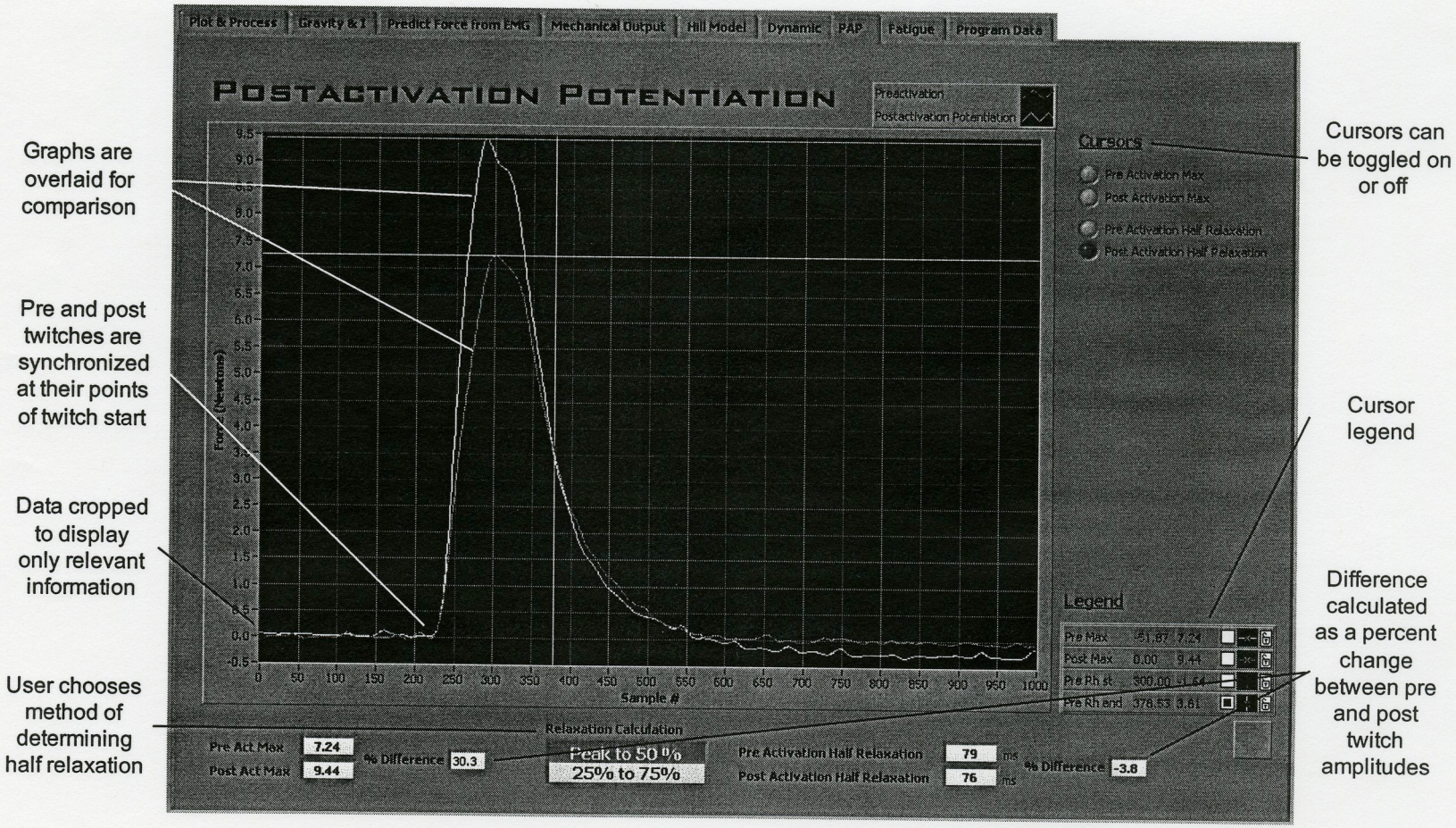

Figure 4-23 Postactivation Potentiation User Interface Panel

This module was added to provide additional estimates of muscle structure. The information gained is not used for the torque-EMG model.

Postactivation potentiation (PAP) is the name for the phenomenon whereby force of a twitch contraction increases after a brief MVC. Hamada et al. demonstrated a correlation between PAP and fiber type composition in human knee extensor muscles. They confirmed what was known for small mammals, that muscles with predominantly fast twitch fibers show greater PAP than muscles with predominantly slow twitch fibers (Hamada et al. 2000).

One trial of the project measured the evoked twitch before and after a ten second isometric elbow extension MVC at 60°. This module compares the pre and postactivation twitches as shown in Figure 4-24. It calculates the increase in twitch force and the difference in half relaxation times. Half relaxation time can be calculated from twitch peak to 50% of max, or 75% of max to 25% of max as shown in Figure 4-23.

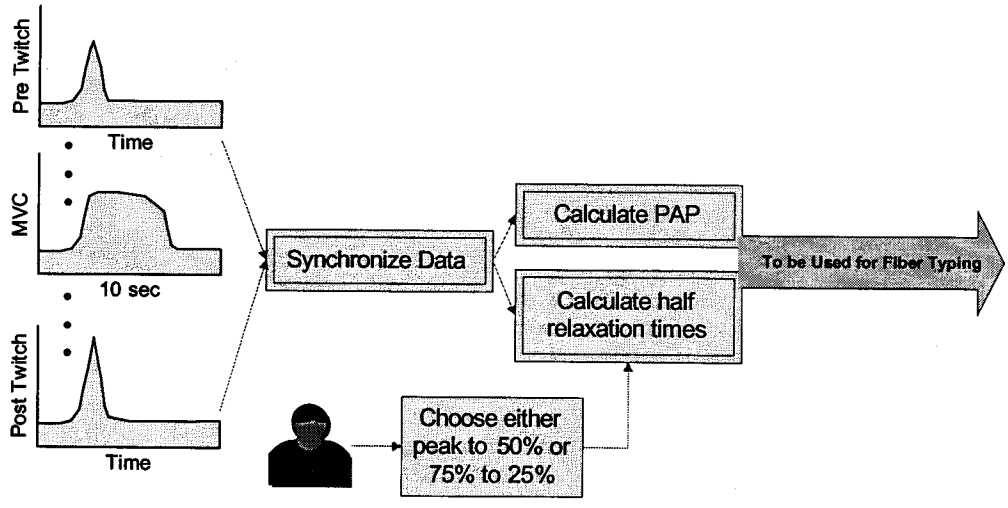

Figure 4-24 Post Activation Potentiation Module Overview

Percent PAP was calculated for each subject and then compared with subjects' maximum angular velocity in order to check for a correlation between fiber type and contraction speed. In this particular study, no correlation was found.

Fatigue Module

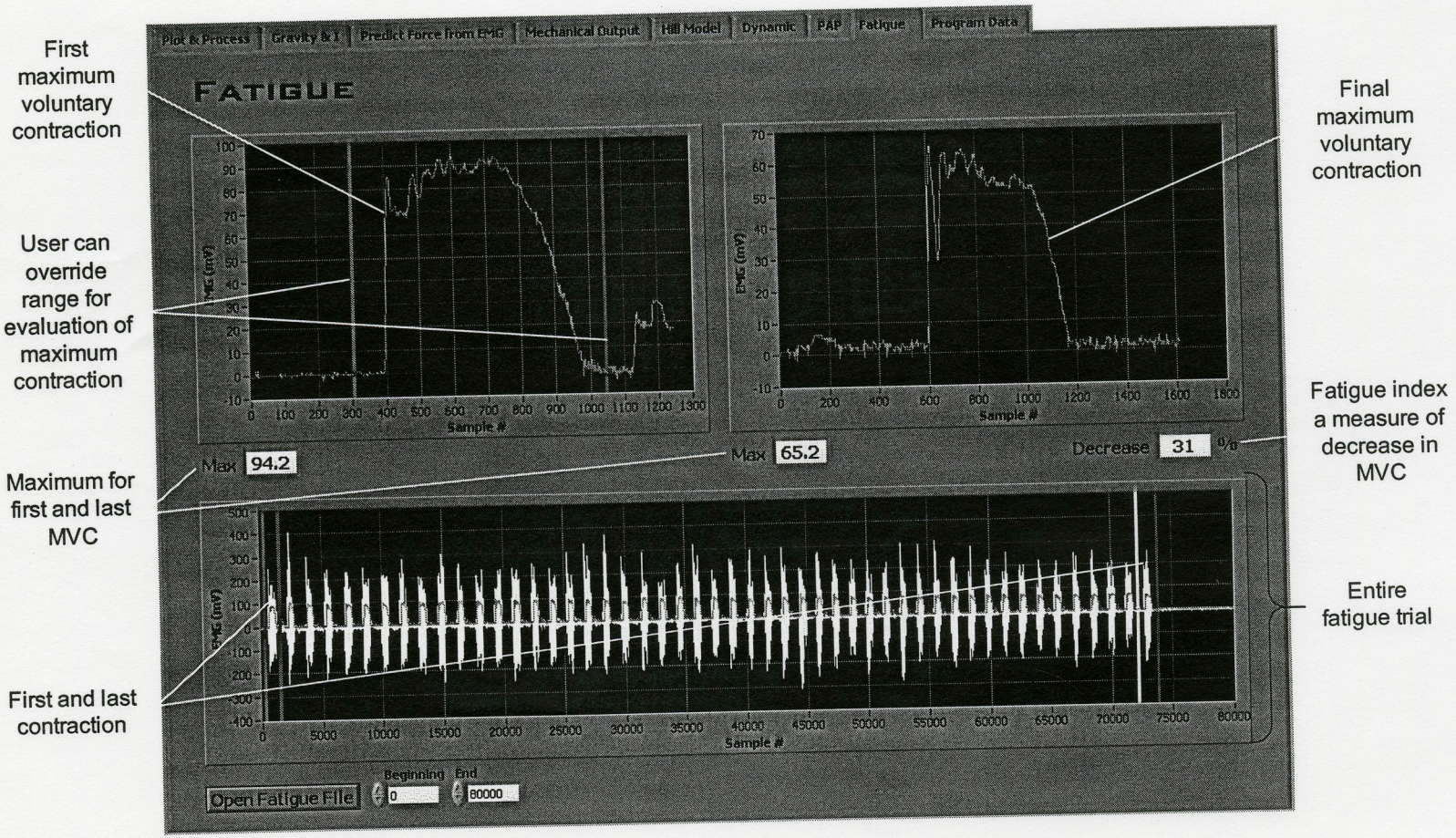

Figure 4-25 Fatigue User Interface Panel

This module is also not used for the torque-EMG model. It was added to provide additional information of muscle function.

An index of fatigue is derived from an isokinetic fatiguing trial. The trial involved 50 maximum elbow extensions on a CYBEX dynamometer. They were performed at a rate of approximately one contraction every 1.5 seconds. This module is designed to isolate the first and the final contraction and subsequently calculate the percent decrease in MVC torque. This percent decrease is used as an index of fatigue. Unprocessed EMG is also displayed for comparison in Figure 4-25.

Program Data Module

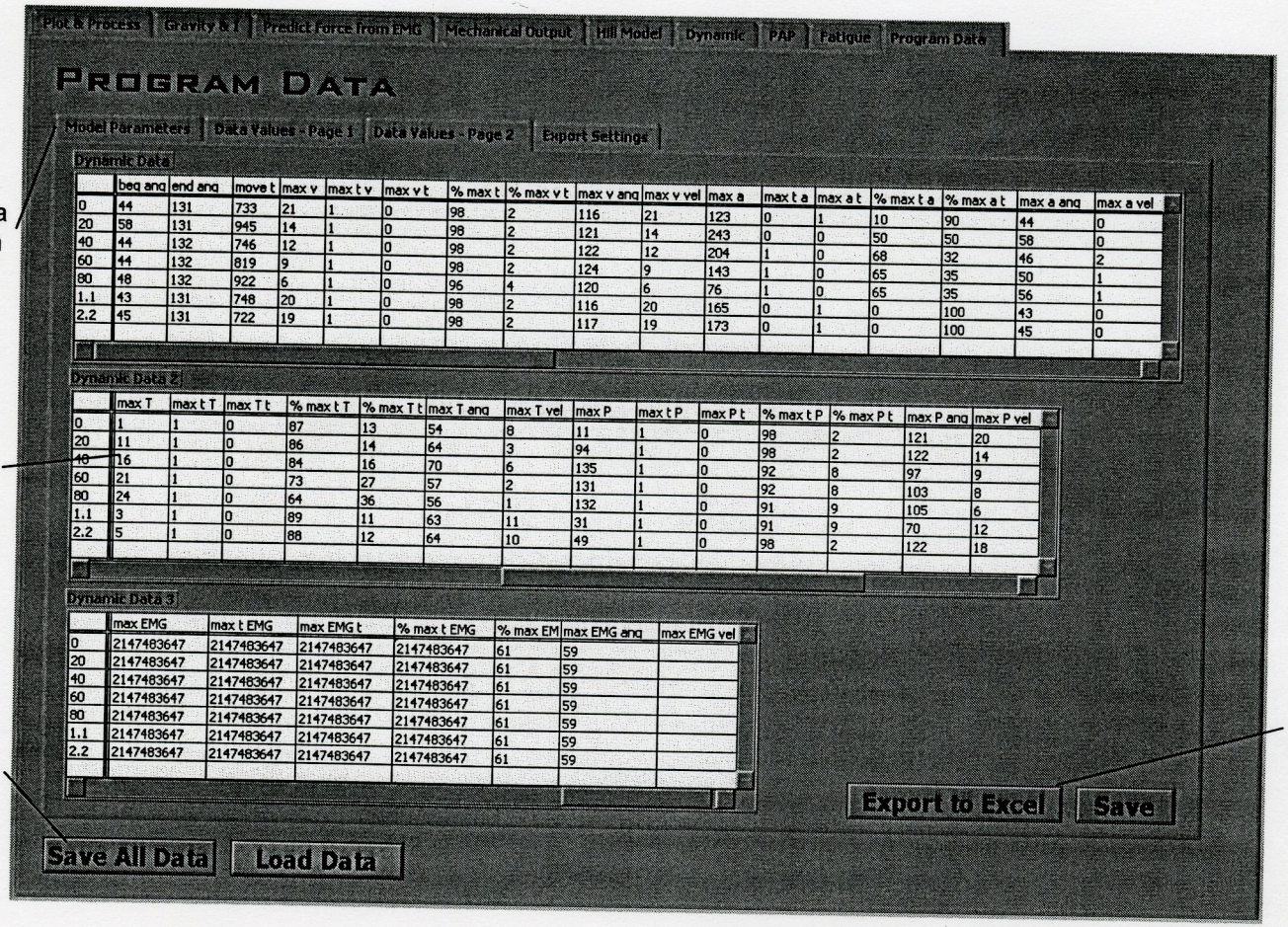

User navigates data by clicking on tabs

Data is updated automatically

This will save all of the program data so that it can be loaded at any time

Program will open Microsoft Excel and export data into a formatted table

Figure 4-26 Program Data User Interface Panel

This final module collects all model parameters as well as calculated values from the entire program. The data is grouped into categories and located on multiple tabbed pages as shown in Figure 4-26. The user can save all or parts of the data, as well as export it to Microsoft Excel into a formatted table.

CHAPTER 5
DISCUSSION AND CONCLUSIONS

The true test of a research tool is how well it performs during actual experiments. This software was developed to analyze data of a particular biomechanics project at McMaster University, and its effectiveness was assessed first hand.

Conclusions derived regarding muscle modeling are best left to the researcher using the software. However, a critical analysis can be made as to how well the software met its design specifications. Several elements stood out among the rest.

Strengths of the Software

Perhaps the most obvious strength of the software package is its capacity both in regard to the volume of raw data it can handle as well as the sheer number of processing steps it can perform. It is difficult to imagine how the same results could have been achieved using spreadsheets and available stand-alone analysis techniques. Even if it were possible, each analysis would require an overwhelming amount of time, be prone to error and require excessive repetition. Furthermore, a single mistake might require re-doing a lot of analysis. During development for example, scaling factors for the torque sensor and angle meter data were changed more than once due to recalibrations of the equipment. In each case, only one value needed to be modified via the keyboard, and all successive processing was automatically altered to reflect the new setting.

Another strength of the program is the ability to visualize each step of the protocol. The user is able to change an input and instantaneously see the results of that change on the processed data. The benefits of this are threefold. Firstly, the user can quickly verify that experimental data was collected properly by running through the most important processing before taking time to fine tune the calibration of all parameters. In this way, aberrations such as equipment failure can be detected early. Secondly, the user has very precise control over all aspects of data processing. Thirdly, the user is given the ability to "play" with the data and evaluate alternate processing techniques.

This benefit was best demonstrated within the Isometric Torque Prediction module. Whenever the user was unsure of chosen filter cutoff for EMG linear envelope, different frequencies could be directly evaluated by dragging the mouse cursor over a vertical slide bar. The program loops continuously and instantaneously displays the effects of each change.

On one occasion, raw data visualization helped the researchers discover that halfway through the experiment, a gain setting on the torque meter amplifier was inadvertently changed. Data from different subjects was easily compared in the Plot and Process module to determine which trials had been affected. The error was quickly fixed.

On another occasion, data visualization and manipulation in the Mechanical Analysis module helped to expose an equipment design flaw. Torque measurements during dynamic contractions showed an undulation inconsistent with expected smooth output curves. The software made it easy to compare dynamic trials of different

individuals. Such comparisons resulted in clues that ultimately lead to an examination of the experimental setup and to the discovery of the source of the unexpected undulations.

Overall, the software's processing capacity and data visualization aid the user in developing innovative approaches to biomechanics analysis – this may be its biggest asset.

Limitations of the Software

The high degree of program flexibility calls for a high degree of responsibility from the user to respect the limitations of data analysis. The easier it is to process data, the greater the tendency to overuse the available tools. Due to the complexity of the program, inexperienced researchers may gain overconfidence in their ability to draw significant conclusions.

In the case of this experiment, error propagation was in fact not considered. The experiment rendered only qualitative insights into muscle modeling. On their own, each module produced acceptable values for model variables. Respecting the error from module to module however was left to the discretion of the researcher. Smooth transitions between modules may have lead to the illusory assumption that there is no propagation of error. When all model variables were brought together to predict torque in dynamic trials, the researcher decided to make many manual subjective adjustments to the variables in order to match the modeled torque with the measured torque. Furthermore, the manual adjustments were not consistent between subjects, thereby complicating any comparisons of models between subjects. Without a measure of significance, conclusions were difficult to justify.

Future Considerations

The key to future work is to create a program that can be used for different biomechanics experiments. Although this software was written with one particular elbow extension experiment in mind, it was created in modules with the idea that it may one day be modified to fit more general applications. As it stands, the modules are designed to execute sequentially.

Figure 5-1 shows a proposed user interface panel for a future version of the software.

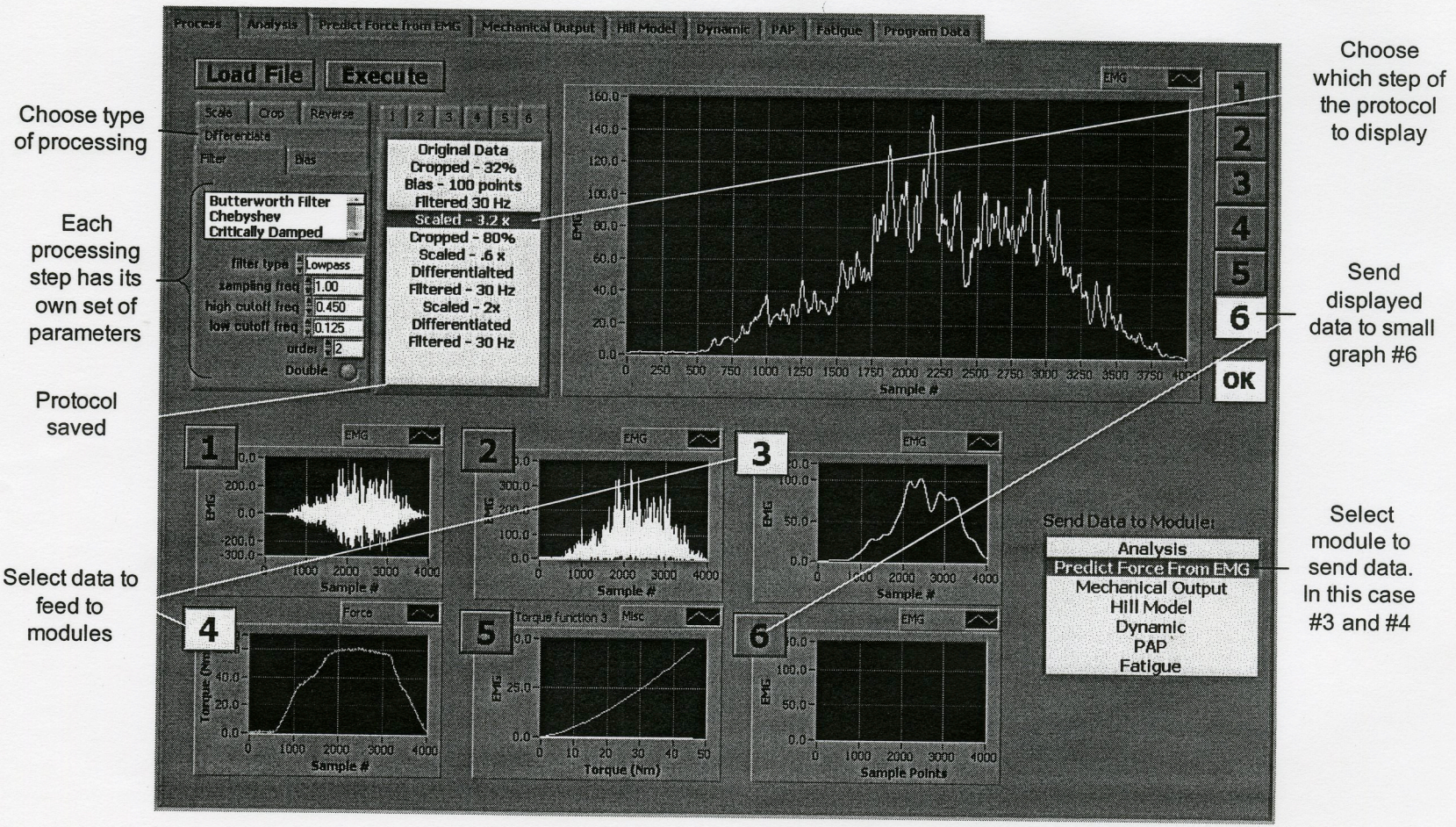

Figure 5-1 User Interface for Proposed Software

The first step to programming would be to isolate the modules by standardizing the format of input and output data. Secondly, controls would have to be added to each module to allow the user freedom to choose which data are to be used as input. The idea is to allow each module to operate as a stand-alone program. Additionally, small processing subroutines would be written to allow for basic data processing such as scaling, cropping and filtering. An overall data flow control module would integrate the stand-alone modules with the small processing subroutines. Ideally the user would have full control over which module and which processing subroutine to use. Processing protocols could be designed "on the fly" by deciding on the number and order of processing steps. Figure 5-2 shows the proposed data flow for such a module.

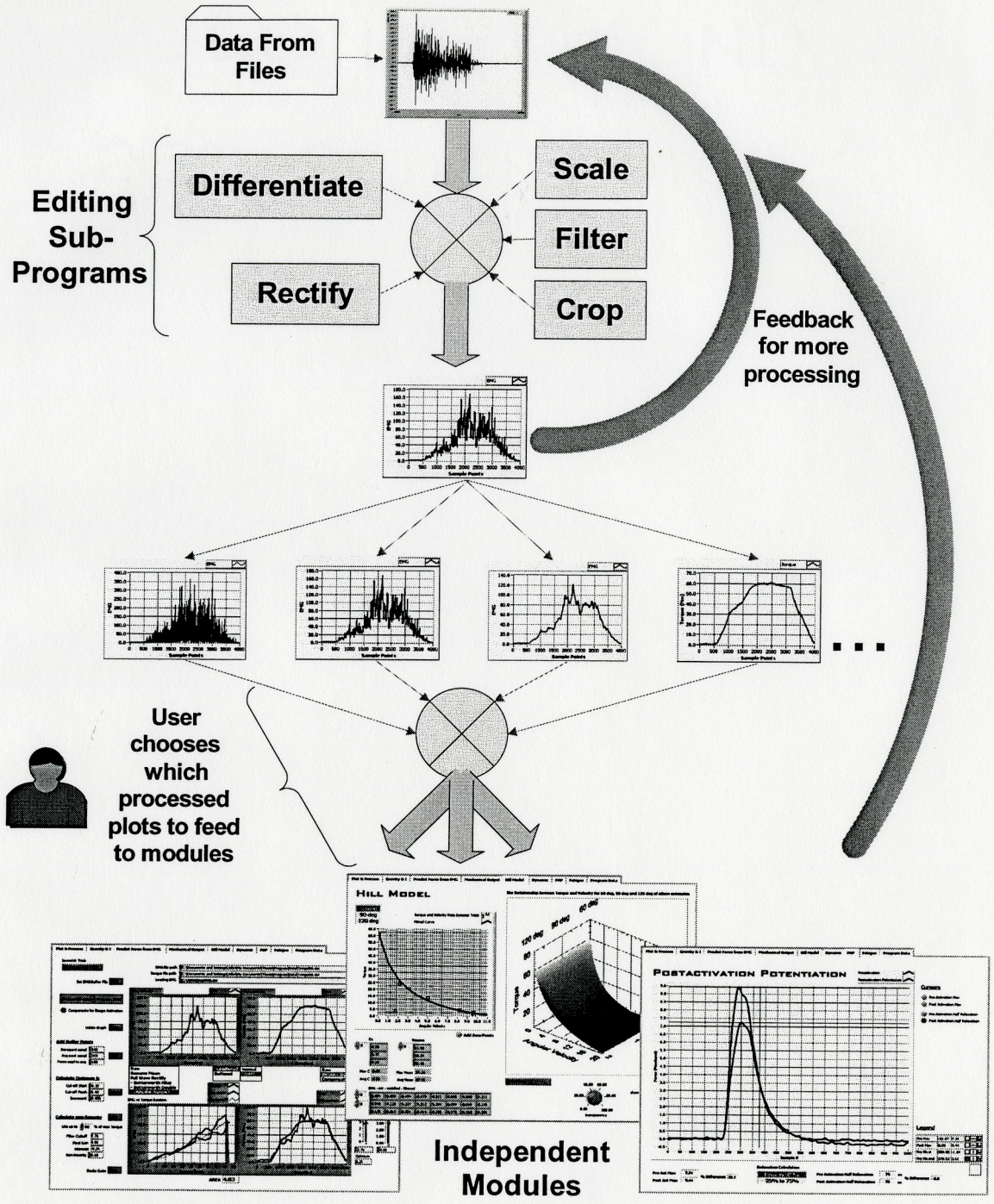

Figure 5-2 Data Flow Diagram for Proposed Software

Other future considerations may be to add statistical analysis capabilities to the existing modules. This may give the user a sense of variance and of error propagation.

Finally, if the software is ever to be exposed to a broader user base such as other research institutions, it must be modified for maximum intuitive use and user friendliness as well as be rigorously tested for bugs and software errors.

APPENDIX
LABVIEW CODE EXAMPLES

The following are examples of the graphical programming environment of LabVIEW. These three screens represent only a very small fraction of the total code.

Data Flow

Code is grouped in nested sequence diagrams on multiple pages

Data flow indicated by connected wires

The program runs continuously so the user can see the results of inputs immediately

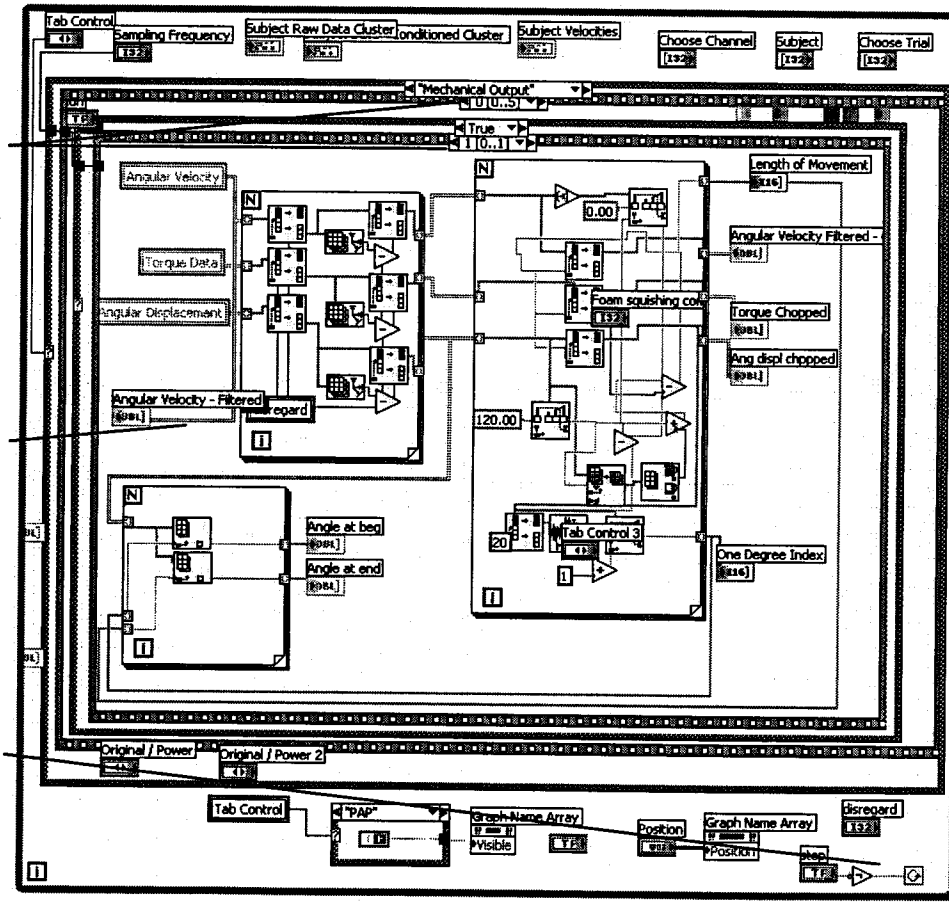

Data Structures and Functions

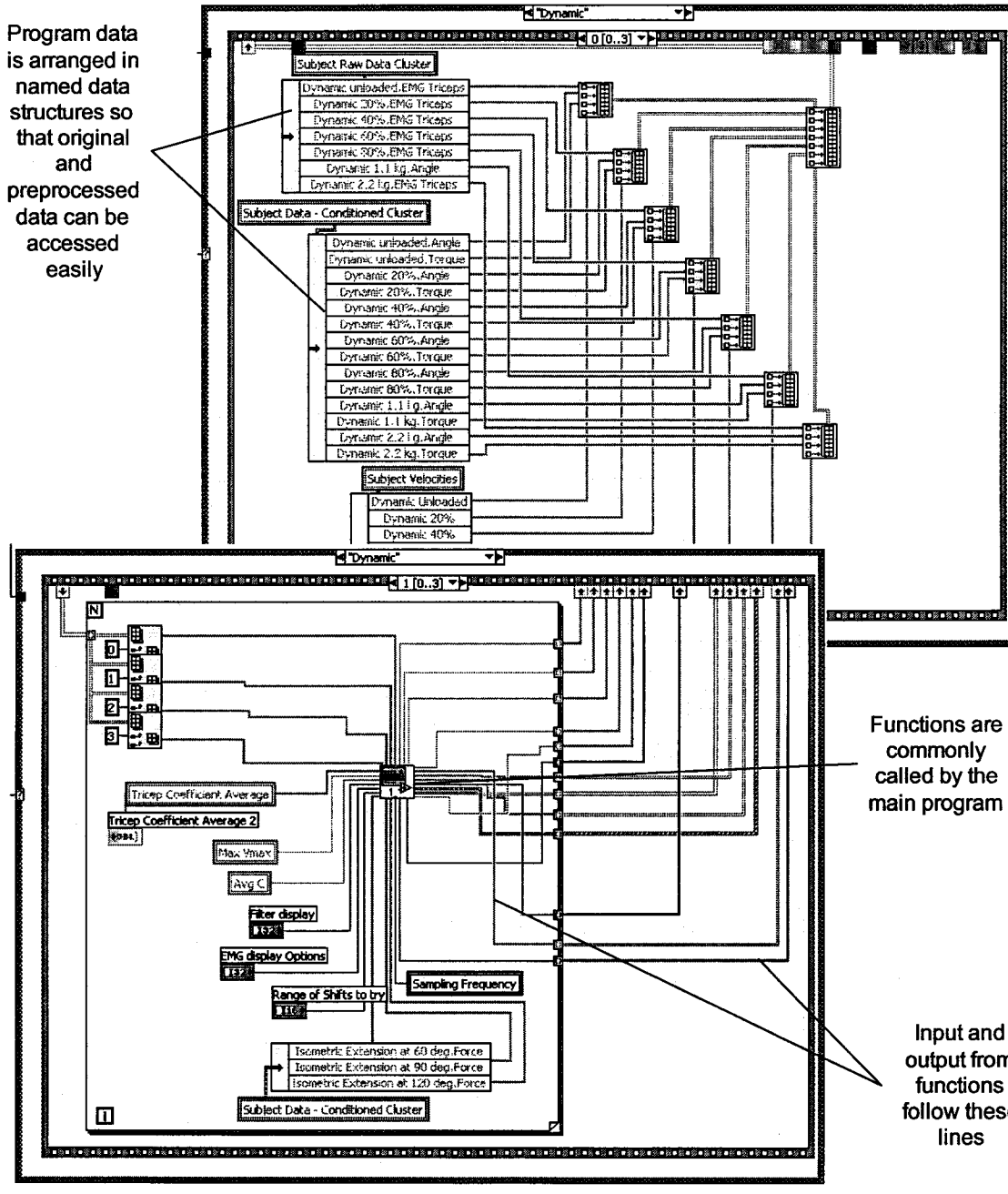

LIST OF REFERENCES

Adrian, E. D., and D. W. Bronk. 1929 The Discharge of Impulses in Motor Nerve Fibers. Part II The Frequency of Discharge in Reflex and Voluntary Contractions. *Journal of Physiology* 67: 119-151

Bodine-Fowler, S., A. Garfinkel, R. R. Roy, and V. R. Edgerton. 1990 Spatial Distribution of Muscle Fibers within the Territory of a Motor Unit. *Muscle & Nerve* 13: 1133-1145

Broman, H., G. Bilotto, and C. J. De Luca. 1985 Myoelectric Signal Conduction Velocity and Spectral Parameters: Influence of Force and Time. *Journal of Applied Physiology* 58(5): 1428-1437

Brooke, M. H., K. K. Kaiser. 1970 Three "Myosin Adenosine Triphosphatase" Systems. The Nature of their pH Lability and Sulfhydryl Dependence. *Journal of Histochemisty and Cytochemisty* 18: 670-672

Buchthal, F., C. Guld, and P. Rosenfalck 1954 Action Potential Parameters in Normal Human Muscle and their Dependence on Physical Variables. *Acta Physiologica Scandinavica* 32: 200-218

Buchthal, F., C. Guld, and P. Rosenfalck. 1955 Innervation Zone and Propagation Velocity in Human Muscle. *Acta Physiologica Scandinavica* 35: 174-190

Buchthal, F., C. Guld, and P. Rosenfalck. 1957 Multielectrode Study of the Territory of a Motor Unit. *Acta Physiologica Scandinavica 39: 84-104*

Buchthal, F., Pinelli, and P. Rosenfalck. 1954 Action Potential Parameters in Normal Human Muscle and their Physiological Determinants. *Acta Physiologica Scandinavica* 32: 219-229

Burke, R. E., D. N. Levine, P. Tsairis, and F. E. Zajac. 1973 Physiological Types and Histochemical Profiles in Motor Units of the Cat Gastrocnemius. *Journal of Physiology* 234: 723-748

De Luca, C. J. 1997 The Use of Surface Electromyography in Biomechanics. *Journal of Applied Biomechanics* 13: 135-165

Dumitru, D, and J. A. DeLisa. 1991 AAEM Minimonography #10: Volume Conduction. *Muscle & Nerve* 14: 605-624

Edwards, R. H. T., D. K. Hill, D. A. Jones, and P. A. Merton. 1977 Fatigue of Long Duration in Human Skeletal Muscle after Exercise. *Journal of Physiology* 272: 769-778

Enoka, R. M., G. A., Robinson and A. R. Kossev. 1989 Task and Fatigue on Low-Threshold Motor Units in Human Hand Muscle. *Journal of Neurophysiology* 62(6): 1344-1359

Fuglevand, A. J., D. A. Winter, and A. E. Patla. 1993 Models of Recruitment and Rate Coding Organization in Motor-Unit Pools. *Journal of Neurophysiology* 70(6): 2470-2488

Gilson Jr., A. S., and W. B. Mills. 1941 Activities of Single Motor Units in Man During Slight Voluntary Efforts. *American Journal of Physiology* 133: 658-669

Gootzen, T. H. J. M., D. F. Stegeman, and A. Van Oosterom. 1991 Finite Limb Dimensions and Finite Muscle Length in a Model of the Generation of Electromyographic Signals. *Electromyography and Clinical Neurophysiology* 81: 152-162

Gordon, A. M., A. F. Huxley and F. J. Julian. 1964 The Length-Tension Diagram of Single Vertebrate Striated Muscle Fibers. *Proceedings of the Physiological Society – Royal College of Surgeons Meeting - Journal of Physiology* 171: 28P-31P

Gydikov, A. 1981 Spreading of Potentials Along the Muscle Investigated by Averaging of the Summated EMG. *Electromyography and Clinical Neurophysiology* 21: 525-538

Gydikov, A., K. Kostov, A. Kossen, and D. Kosarov. 1984. Estimation of the Spreading Velocity and the Parameters of the Muscle Potentials by Averaging of the Summated Electromyogram. *Electromyography and Clinical Neurophysiology* 24: 191-212

Hamada, T., D. G. Sale, J. D. MacDougall, and M. Tarnopolsky. 2001 Postactivation Potentiation, Fiber Type, and Twitch Contraction Time in Human Knee Extensor Muscles. *Journal of Applied Physiology* 88: 2131-2137

Hamm, T. M., R. M., Reinking and D. G. Stuart. 1989 Electromyographic Responses of Mammalian Motor Units to a Fatigue Test. *Electromyography and Clinical Neurophysiology* 29: 485-494

Hof, A. L., and Jw. Van den Berg. 1981a EMG to Force Processing I: An Electrical Analogue of the Hill Muscle Model. *Journal of Biomechanics* 14 (11): 747-758

Hof, A. L., and Jw. Van den Berg. 1981b EMG to Force Processing II: Estimation of Parameters of the Hill Muscle Model for the Human Triceps Surae by Means of Calfergometer *Journal of Biomechanics* 14 (11): 759-770

Hof, A. L., and Jw. Van den Berg. 1981c EMG to Force Processing III: Estimation of Model Parameters for the Human Triceps Surae Muscle and Assessment of the Accuracy by Means of a Torque Plate. *Journal of Biomechanics* 14 (11): 771-785

Hof, A. L., and Jw. Van den Berg. 1981d EMG to Force Processing IV: Eccentric-Concentric Contractions on a Spring Flywheel Set Up. *Journal of Biomechanics* 14 (11): 787-792

Hill, A. V. 1937 Methods of Analysing the Heat of Production of Muscle. *Proceedings of the Royal Society – Series B* 125: 114-127:

Hill, A. V. 1938 The Heat of Shortening and the Dynamic Constants of Muscle. *Proceeding of the Royal Society - Series B* 126: 136-195.

Huxley, A. F., and R. Niedergerke 1954. Structural Changes in Muscle During Contraction - Interference Microscopy of Living Muscle Fibers. *Nature* 173: 971-973

Huxley, A. F., 1957. Muscle structure and Theories of Contraction. *Progress in Biophysics and Biophysical Chemistry* 7: 257-318

Huxley, A. F., and R. M. Simmons. 1971 Proposed Mechanism of Force Generation in Striated Muscle. *Nature* 233: 533-538

Huxley, H. E., and J., Hanson. 1954 Structural Changes in Muscle During Contraction - Changes in the Cross-Striations of Muscle During Contraction and Stretch and their Structural Interpretation. *Nature* 173: 973-976.

Inman, V. T., H. J. Ralston, J. B. de C. M. Saunders, B. Feinstein, and E. W. Wright. 1952 Relation of Human Electromyogram to Muscular Tension. *Electroencephalography & Clinical Neurophysiology* 4: 187-194

Kernell, D. 1992 Organized Variability in the Neuromuscular System: A Survey of Task-Related Adaptations. *Archives Italiennes de Biologie* 130: 19-66.

Kukula, C. G., H. P. Clamann. 1981 Comparison of the Recruitment and Discharge Properties of Motor Units in Human Brachial Biceps and Adductor Pollicis Suring Isometric Contractions. *Brain Research* 219: 45-55.

Lindström, L., R. Magnusson, and I. Petersén. 1974 Muscle Load Influence on Myoelectric Signal Characteristics. *Scandinavian Journal of Rehabilitation Medicine. Supplement* 3: 127-148

Lippold, O. C. J. 1952. The Relation Between Integrated Action Potentials in a Human Muscle and its Isometric Tension. *Journal of Physiology* 117: 492-499

Masuda, T., H. Miyano, and T. Sadoyoma. 1985 The Position of Innervation Zones in the Biceps Brachii Investigated by Surface Electromyography. *IEEE Transactions on Biomedical Engineering* 32(1): 36-42

Masuda, T., H. Miyano, and T. Sadoyoma. 1983 The Propagation of Motor Unit Action Potential and the Location of Neuromuscular Junction Investigated by Surface Electrode Arrays. *Clinical Neurophysiology* 55: 594-600

Mullins, L. J. and K. Noda. 1963 The Influence of Sodium-Free Solutions on the Membrane Potential of Frog Muscle Fibers. *Journal of General Physiology* 47: 117-132

Olney, S. J., D. A. Winter. 1985 Predictions of Knee and Ankle Moments of Force in Walking from EMG and Kinematic Data. *Journal of Biomechanics* 18(1): 9-20

Person, R. S. 1974 Rhythmic Activity of a Group of Human Motoneurons During Voluntary Contraction of a Muscle. *Electroencephalography and Clinical Neurophysiology* 36: 585-595

Person, R. S. and L. P. Kudina. 1972 Discharge Frequency and Discharge Pattern of Human Motor Units During Voluntary Contraction of Muscle. *Electroencephalography and Clinical Neurophysiology* 32: 471-483

Rosenbleuth A., J. H. Wills, and H. Hoagland. 1941 The Slow Components of the Electromyogram of Striated Muscle. *American Journal of Physiology* 133: 724-735

Sherif, M. H., R. J. Gregor, L. M. Liu, R. R. Roy, and C. L. Hager. 1983 Correlation of Myoelectric Activity and Muscle Force During Selected Cat Treadmill Locomotion. *Journal of Biomechanics* 16(9): 691-701

Sherrington, C. S. 1925 Remarks on Some Aspects of Reflex Inhibition. *Proceedings of the Royal Society – Series B* 97:519-545

Siegler, S., H. J. Hillstrom, W. Freedman, and G. Moskowitz. 1985. Effect of Myoelectric Signal Processing on the Relationship Between Muscle Force and Processed EMG. *American Journal of Physical Medicine* 64(3): 130-149

Zuniga, E., D. G. Simons. 1969 Nonlinear Relationship Between Averaged Electromyogram Potential and Muscle Tension in Normal Subjects. *Archives of Physical Medicine & Rehabilitation* 50: 613-620